Materials and Structures manuscript No.
(will be inserted by the editor)

Shrinkage of recycled aggregate concrete

Experimental database and application of *fib* Model Code 2010

Nikola Tošić · Albert de la Fuente · Snežana Marinković

Received: date / Accepted: date

Abstract This paper describes a meta-analysis of previously published studies on the shrinkage strain of recycled aggregate concrete (RAC). The study aims at providing an analytic expression for the shrinkage strain of RAC to be used in conjunction with the existing *fib* Model Code 2010 shrinkage prediction model. For this purpose, a database of experimental results on the shrinkage of RAC and companion natural aggregate concrete (NAC), produced with the same water-cement ratio, was compiled using strict selection criteria. Results from 19 studies entered into the database, consisting of 125 shrinkage curves (39 NAC and 86 RAC) with a total of 424 data points. A comparison of RAC and companion NAC revealed that, on average, RAC displays a larger shrinkage strain. This difference increases with increasing recycled concrete aggregate (RCA) content and with decreasing compressive strength. Applying the *fib* Model Code 2010 shrinkage prediction model revealed that, relative to its performance on NAC, the shrinkage strain of RAC is underestimated. Finally, a correction coefficient for the shrinkage strain of RAC, $\xi_{cs,RAC}$, to be used in conjunction with the *fib* Model Code 2010 model, was proposed in the form of a bivariate power function with RAC compressive strength and RCA replacement ratio as variables.

Keywords Recycled concrete aggregate · Recycled aggregate concrete · Shrinkage · Database · Model Code

1 Introduction

Shrinkage of concrete, i.e. the time-dependent volumetric change of unloaded concrete at a constant temperature, has been studied extensively since it was first observed 130 years ago [27]. Because of the significant effects it can have on the behaviour of concrete structure,

N. Tošić · S. Marinković
University of Belgrade, Faculty of Civil Engineering, Bulevar kralja Aleksandra 73, 11000 Belgrade, Serbia
Tel.: +381 11 3218 547
Fax: +381 11 3370 253
E-mail: ntosic@imk.grf.bg.ac.rs

A. de la Fuente
Civil and Environmental Engineering Department, Universitat Politécnica de Catalunya (UPC), Jordi Girona 1-3, 08034 Barcelona, Spain

e.g. causing cracking or imposed deformations in restrained members that could result in additional stresses, the interest of both the scientific and technical communities into shrinkage of concrete has been increasing since the 1960s.

Starting from purely empirical observations on a macro-level, over time, researchers have become able to study concrete shrinkage at micro and nano scales, separating it into different components, viz. autogenous, and drying shrinkage [29], and explaining it with increasingly complex theories, through capillary tension and removal of intercrystalline water from pores, diffusion, etc. [6, 37]. On the level of engineering applications and design of concrete structures, prediction models for calculating shrinkage strain have also become more complex. Whereas older models, such as the ACI 209R-92 or *fib* Model Code 1990 models [2, 12], de facto only considered drying shrinkage and their mathematical form was that of a simple multiplication of influencing parameters, current advanced models, such as the *fib* Model Code 2010 (MC2010) and B4 models [20, 7], separate shrinkage strain into autogenous (basic) and drying components and have complex mathematical formulations.

What allowed such a rapid advance and development was the substantial effort put in by researchers to compile databases of experimental results. Databases of results of concrete shrinkage and creep now have a tradition of over 50 years. The first database was prepared in the 1960s for the first CEB-FIP Model Code and its shrinkage and creep model [11]. Afterwards, another one was compiled for the 1971 ACI 209 model [2]. These efforts were continued in the 1970s at the Northwestern University within the work on the BP model [5]. The work was expanded through a subcommittee of the RILEM Committee TC107, chaired by professor Harald S. Müller. This led to the creation of the RILEM-ACI 209 Database in 1992, subsequently expanded in 2008 and 2010 [24].

The most recent version of the database, the 'NU-ITI database on concrete creep and shrinkage' was assembled in 2010–2013 at the Northwestern University's Infrastructure Technology Institute, mainly through the support from the U.S. Department of Transportation. The database is freely available online [23]. The information in this database was mostly extracted from numerous journal articles, conference proceedings and reports [24]. The final version of the NU-ITI database contains 1751 shrinkage curves (1217 'total', 417 autogenous and 117 drying shrinkage curves).

Even at such a large number of experimental results, the database still has several deficiencies: most of the data in the database is crowded into short test durations (there are no tests exceeding 6 years while the mean test duration is 180 days), most of the tested specimens are crowded into small thicknesses, and the variability in the database is dominated by differences in concrete composition, aggregate type, and admixture effects [24]. Nonetheless, the database is indispensable when testing shrinkage models: using individual tests to evaluate the shape of the predicted shrinkage curves and using the whole database for global statistical analysis and parameter calibration [24].

Although the NU-ITI database attempts to fill some missing gaps in terms of concrete composition, such as incorporating concretes with very low water-cement (*w/c*) ratios and concretes which rely heavily on cement replacement and admixtures, there is no information on the shrinkage behaviour of recycled aggregate concrete (RAC), even though RAC produced with coarse recycled concrete aggregate (RCA) is one of the most studied and most promising green concretes. The aim of this study is to fill in this gap.

Various researchers have studied the shrinkage of RAC in differing ways, trying to identify ways in which RCA affects shrinkage: one way this effect is achieved is through the stiffness of RCA, since aggregate stiffness provides the major source of restraint to shrinkage; another important factor however, is the residual cement paste on RCA particles, part of which can be unhydrated [19]. It can have a complex influence on these phenomena

through its porosity, volume fraction, quality, etc. Over the years, the amount of research on RAC shrinkage has become significant – there now exist several literature reviews and meta-analyses.

One of the largest reviews is the study by Lye et al. [28] – the authors initially identified 286 studies in English published since 1978 containing experimental results on concretes produced with various recycled materials. Upon filtering this database down to RAC produced with coarse RCA, the authors reported 118 studies [28]. All of the studies are comparisons between the shrinkage strain of RAC and a 'companion' natural aggregate concrete (NAC), defined as having the same *w/c* ratio as RAC. The main conclusion from this, and other similar studies, is that, on average, RAC displays greater shrinkage than companion NAC and that this difference increases with increasing RCA content (replacement ratio) and with decreasing compressive strength [28, 34, 25]. For instance, there exists a general agreement that for a normal strength RAC with 100% coarse RCA, the average expected increase in shrinkage strain relative to a companion NAC will be 30–40% [28, 34, 25].

What is still lacking, however, are useful analytic expressions for predicting the shrinkage strain of RAC, built upon existing models. In this regard, the study by Lye et al. [28] offers a useful first step. From their database, the authors constructed diagrams for determining correction factors for RAC shrinkage strain applicable to the Eurocode 2 model [17]. The diagrams are a family of curves, defined by the RCA replacement ratio in RAC (0–100%) and RAC compressive strength (20–130 MPa). The shrinkage strain calculated by Eurocode 2 (for a given compressive strength of RAC) only needs to be multiplied by the correction factor derived from the graphs. While easily understandable, the use of diagrams is not easily applicable to computer-based design and requires manual calculation. Additionally, there is room for improvement in selection criteria applied to the database in [28].

The first aim of this study is to compile a new database of experimental results on the shrinkage strain of RAC and companion NAC using strict and clear selection criteria. The second aim is to formulate an analytic expression for a correction coefficient for RAC shrinkage strain applicable to the MC2010 shrinkage model [20] through a statistical meta-analysis of the database. The reason for choosing MC2010 instead of Eurocode 2 is the fact that the former is a more advanced shrinkage prediction model which will form the basis for the new version of Eurocode 2, currently in preparation.

2 RAC shrinkage database

2.1 Compilation of database

The first step in this study was the compilation of a new database of experimental results on RAC and companion NAC shrinkage. As previously mentioned, several authors have already conducted literature reviews on the topic and compiled similar databases [28, 34, 25]; however, since the aim of this study was not only to compare shrinkage strain between RAC and NAC, but also to analyse the applicability of the MC2010 model, a stricter approach in selecting studies for the database was needed.

Strict and clear criteria were needed for the selection process. In order to enter into the database, every study had to fulfill the following criteria:

- results are given on the shrinkage strain of RAC *and* companion NAC defined as having the same *w/c* ratio;
- 28-day compressive strength is provided along with the type of test specimen used for testing it;

- the *w/c* ratio is provided;
- water absorption (*w.a.*) of coarse aggregates is provided;
- any reactive additives, such as fly ash, are used in amounts smaller than 30% of cement;
- curing time of shrinkage specimens t_s, their dimensions or notional size h_0 (two times the ratio of a cross-section's area to its perimeter in contact with the atmosphere, $2 \cdot A_c/u$), and the ambient conditions during testing are provided; and
- shrinkage strain values are reported for at least two points in time $t - t_s$, i.e. the results are given in the form of a 'shrinkage time curve'.

It can be seen from the criteria that the information they require allows for a meaningful comparison of RAC and companion NAC shrinkage, since all important influencing factors are experimentally reported. **The only assumption which was made when data was missing was regarding the type of cement used: since it was found that a significant number of studies does not report it, in such cases it was assumed as 42.5N for both RAC and NAC.**

Probably the most important difference between a database like this one and those from previous studies, is that, in this one, shrinkage time curves were studied as the basic unit of analysis and not single 'final' shrinkage strain values [28, 34, 25]. Thus, deeper analyses are possible, such as comparing possibly different kinetics of the shrinkage process in RAC and companion NAC, as well as testing entire predicted time curves by any model, i.e. models' accuracy over the entire drying period.

Following the final criterion of at least two shrinkage values reported for each mixture, in the majority of studies, values were not given in tabular but rather in graphical form. In such cases, the figures with shrinkage curves were imported into a CAD software, scaled appropriately and values were read of the graphs. **Shrinkage time curves were obtained by 'sampling' as equally as possible from each 'time decade' covered by the reported shrinkage curve (1–9.9, 10–99.9, 100—999.9, 1000– days) and also, by sampling as equally as possible between different experiments – the aim was to always sample at certain drying times, e.g. 28, 90, 180 days. Importantly, within the same experiment, RAC and companion NAC shrinkage curves were always sampled at the same ages.**

The compilation of the database consisted of going through studies reported in previous literature reviews [28, 34, 25] and applying these criteria. In the end, 19 studies entered into the database [8, 9, 10, 13, 16, 21, 22, 36, 38, 4, 14, 15, 18, 26, 30, 33, 35, 39, 32] with a total 125 shrinkage time curves (39 NAC and 86 RAC), consisting of 424 data points. Only one of the studies investigated autogenous and drying shrinkage separately [21]. Hence, all further analyses and discussion will be concerned with *total* shrinkage strain.

In comparison with the database created by Lye et al. [28] with 118 studies, the database presented in this paper contains a significantly smaller number of studies, i.e. only 19. However, the criteria used herein are much stricter as practically no missing information was allowed. For example, in [28], a large number of studies are conference proceedings and these typically lack some of the necessary information due to their brevity. Most often, the missing information are the ambient conditions during the shrinkage test, i.e. relative humidity (RH), or specimen size. Other studies do not report the water absorption of RCA or they only provide a single 'final' shrinkage strain. The full database Excel file is available as Online Resource 1 and the ranges of the most important parameters of the database are given in Table 1 with their mean values given in parentheses.

As seen from the database, the ranges of parameters and their means for RAC and companion NAC are very similar, except for water absorption of aggregates. The values cover the entire range of 'normal' compressive strengths (20–60 MPa) and usual *w/c* ratios for these

Table 1 Range of parameters in the database

		No. of curves	No. of points	f_{cm} (MPa)	w/c (–)	$w.a.$ (%)	$t-t_s$ (days)	h_0 (mm)	RH (%)
NAC		39	133	20–61 (40.9)	0.40–0.73 (0.53)	0.3–3.0 (1.65)	1–1000 (100)	25–75 (55)	48–80 (58)
RAC	1–25%	11	44	29–54 (45.4)	0.43–0.65 (0.54)	4.6–7.0 (5.8)	7–1000 (164)	38–75 (65)	50–75 (61)
	26–50%	21	86	26–52 (38.8)	0.40–0.65 (0.51)	4.8–7.5 (6.3)	7–1000 (117)	25–75 (57)	50–80 (57)
	51–75%	2	7	27–38 (31.4)	0.50–0.52 (0.51)	4.8–6.3 (5.6)	28–270 (127)	50–75 (64)	50–65 (56)
	76–100%	52	154	19–56 (35.3)	0.43–0.75 (0.55)	1.9–7.0 (5.2)	1–1000 (91)	25–75 (53)	48–80 (61)

Note: values in parentheses represent mean values of respective ranges

concretes. The range of parameters for RAC has been classified according to the coarse RCA content – most of the data are on RAC with 100% of RCA, followed by contents around 50% and 25%; there is a notable lack of data on RAC with 51–75% of RCA and this range of replacement percentages offers less room for analysis.

The water absorption of RCA ranges from 1.9 to 7.5 and any conclusion of this study is only valid for RCA with absorption in this range. However, the notional sizes of the specimens are small compared with full-scale structures and this has to be kept in mind. **The duration of the measurements does not go beyond 1000 days, except in one study [32]. The mean test duration for the entire database is just above 180 days (whereas the mode is 90 days) and 90% of the tests are shorter than 270 days.**

2.2 Comparison of RAC and companion NAC

The next step in this study was to directly compare the shrinkage behaviour of RAC and companion NAC mixtures in order to determine whether indeed there are significant differences between them and, if so, what are the parameters influencing these differences.

The simplest way to do this is to form a ratio of RAC-to-NAC shrinkage strain, $\frac{\varepsilon_{cs,RAC}}{\varepsilon_{cs,NAC}}$. **The database provides a total of 291 $\frac{\varepsilon_{cs,RAC}}{\varepsilon_{cs,NAC}}$ ratios (the number of data points for RAC).In other words, the $\frac{\varepsilon_{cs,RAC}}{\varepsilon_{cs,NAC}}$ ratio was calculated for each data point, not only for the 'final shrinkage' values. This was possible because RAC and companion NAC shrinkage curves were always sampled in the same way, i.e. at identical ages.**

The first step was to analyse the statistical descriptors for the $\frac{\varepsilon_{cs,RAC}}{\varepsilon_{cs,NAC}}$ ratio, i.e. its mean and standard deviation or coefficient of variation (CoV). These statistics are given in Table 2 under 'full database'. For RAC with 1–25% of RCA the increase in shrinkage is small, under 10%, with a relatively low CoV. The mean $\frac{\varepsilon_{cs,RAC}}{\varepsilon_{cs,NAC}}$ ratio increases for RAC with 26–50% of RCA with a much larger CoV, decreasing again for RAC with 51–75% of RCA. However, this replacement range has only 7 data points and should not be given equal weight in the analysis. Finally, for RAC with 76–100% of RCA (which are all RAC mixtures with 100% of RCA), the mean $\frac{\varepsilon_{cs,RAC}}{\varepsilon_{cs,NAC}}$ ratio rises sharply to 1.37 and the CoV remains stable, slightly below 25%. This definitely points to an effect of RCA in RAC on the increase in shrinkage strain relative to NAC.

In Figure 1, the $\frac{\varepsilon_{cs,RAC}}{\varepsilon_{cs,NAC}}$ ratios have been plotted against RCA percentage. The ratios can be seen grouped at discrete values of RCA content, e.g. 15%, 20%, 25%, etc. The data are most numerous for RAC with 20%, 30%, 50% and 100% of RCA. The large variability of the $\frac{\varepsilon_{cs,RAC}}{\varepsilon_{cs,NAC}}$ ratio within each RCA percentage can also be seen. **For each RCA percentage,**

Table 2 Statistical descriptors of the $\frac{\varepsilon_{cs,RAC}}{\varepsilon_{cs,NAC}}$ ratio

	Full database		No RAC/NAC outliers	
RCA %	μ	CoV (%)	μ	CoV (%)
1–25	1.08	15.5	1.08	12.1
26–50	1.11	27.9	1.17	19.2
51–75	1.06	23.5	1.06	23.5
76–100	1.37	24.2	1.35	21.9

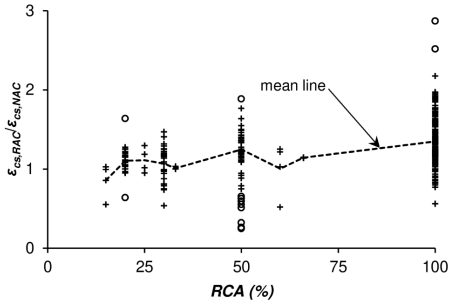

Fig. 1 Distribution of RAC-to-NAC shrinkage strain

a mean value of the $\frac{\varepsilon_{cs,RAC}}{\varepsilon_{cs,NAC}}$ ratio was determined and these are connected by the dashed line in Figure 1, only a slight increasing trend can be noticed. Additionally, in Figure 1, $\frac{\varepsilon_{cs,RAC}}{\varepsilon_{cs,NAC}}$ ratios marked with empty circles can also be seen; these represent outlier ratios identified in each RCA percentage through a box-and-whiskers technique – there are 13 such values: 2, 9, and 2 values for 20%, 50% and 100% of RCA, respectively.

Not considering outliers, the range of values for the $\frac{\varepsilon_{cs,RAC}}{\varepsilon_{cs,NAC}}$ ratio increases with RCA percentage: from 0.949–1.275 for 20% of RCA, to 0.749–1.766 for 50% of RCA, and 0.562–2.177 for 100% of RCA. The statistical descriptors of the database without outliers is given in Table 2 under the heading 'no RAC/NAC outliers'; the reductions in CoVs are also visible.

The differences between RAC and NAC shrinkage can be separated into two types: (1) differences in magnitude and (2) differences in shrinkage development over time. This is illustrated in Figure 2. On the left side of Figure 2, 'vertical scaling' of shrinkage curves is presented. In this case, the kinetics of shrinkage development with time remain identical, only the magnitude of shrinkage changes. This is described by both shrinkage curves having identical shrinkage halftimes τ_h (the time after which half of all shrinkage occurs) but different corresponding shrinkage values $\varepsilon_{cs,h,1}$ and $\varepsilon_{cs,h,2}$. On the right side of Figure 2, 'horizontal scaling' of shrinkage curves is presented. In this case, the final shrinkage values are identical, but the kinetics of shrinkage development with time are different, as described by different shrinkage halftimes $\tau_{h,1}$ and $\tau_{h,2}$.

Therefore, the $\frac{\varepsilon_{cs,RAC}}{\varepsilon_{cs,NAC}}$ ratio can point to both types of differences between RAC and NAC shrinkage. In order to check for 'horizontal' differences between RAC and companion NAC shrinkage, individual shrinkage curves must be checked for any trend in the development of the $\frac{\varepsilon_{cs,RAC}}{\varepsilon_{cs,NAC}}$ ratio with time *within* individual shrinkage curves. For the compiled RAC database, no trend was observed at the level of individual RAC shrinkage curves; the $\frac{\varepsilon_{cs,RAC}}{\varepsilon_{cs,NAC}}$ ratio either remains stable over time or changes randomly.

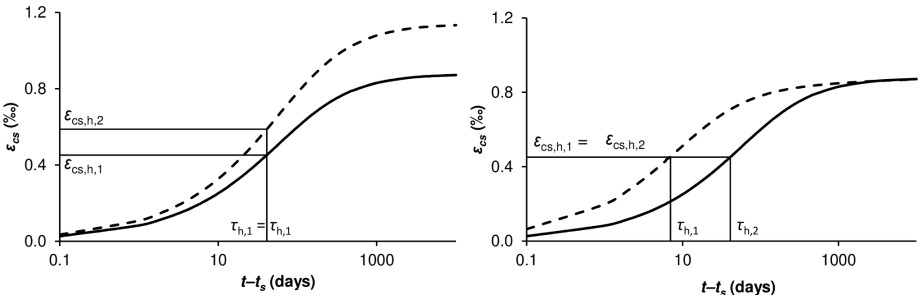

Fig. 2 Differences between vertical (left) and horizontal (right) scaling of shrinkage curves

The average CoV of the $\frac{\varepsilon_{cs,RAC}}{\varepsilon_{cs,NAC}}$ ratio within individual shrinkage curves is just 9%. Thus, no evidence for the need for horizontal scaling can be found, and only vertical scaling of shrinkage magnitude should be considered. Without experimental data separating shrinkage into basic and drying component, a definite conclusion in this regard cannot be drawn. One potential explanation for the result obtained in this study is that the effects of the higher porosity and lower stiffness of RCA, which could lead to faster drying of RAC, are counteracted by the 'internal curing' effect of RCA in which absorbed water is slowly released from RCA particles providing water for hydration and slowing down the drying process [13].

Identifying potential parameters influencing the $\frac{\varepsilon_{cs,RAC}}{\varepsilon_{cs,NAC}}$ ratio is very difficult, as evidenced by the large scatter in Figure 1. Any attempt to do so carries significant bias. In such cases, it can be better to adopt a less statistically-based approach and more of an engineering and practical logic or 'common sense'. Considering the difference between the shrinkage behaviours of RAC and NAC, the question is 'What are potential candidates for influencing parameters?' The influence of parameters like notional size and relative humidity is exerted more on the time evolution of shrinkage, and as said previously, there is currently no strong evidence to support the need for horizontal scaling of RAC shrinkage; to precisely identify the effect of these parameters, more detailed data is needed, specifically separation of RAC shrinkage into autogenous and drying – this is lacking in currently existing results. Some parameters may also be influential and not accounted for by most experiments – pre-saturation of RCA prior to mixing, amount of residual cement paste attached to RCA particles, RCA porosity and stiffness, etc. The remaining option, is to make a pragmatic choice of influencing parameters which should preferably be known in the design stage of an RAC structure, i.e. which it is *reasonable* to know at that stage, and which should by proxy cover as many other parameters as possible.

These conditions are fulfilled by three parameters: RAC compressive strength, f_{cm}, coarse RCA content, *RCA%*, and RCA water absorption, *w.a.*. RAC compressive strength is a proxy value for the *w/c* ratio, stiffness and strength of aggregates and cement paste, density, total cement paste content, etc. Coarse RCA content is also an indirect measure of aggregate stiffness and cement paste content, whereas RCA water absorption describes RCA porosity, density, stiffness and residual cement paste content. In other words, these three parameters are robust and available to an engineer in the design stage (except perhaps RCA water absorption). Even so, the scatter of the data in the database is so large that the correlation coefficient between the $\frac{\varepsilon_{cs,RAC}}{\varepsilon_{cs,NAC}}$ ratio and RAC compressive strength, RCA content

and RCA water absorption is 0.155, 0.411 and -0.136, respectively. To try and illustrate this distribution further, Figures 3 and 4 plot the $\frac{\varepsilon_{cs,RAC}}{\varepsilon_{cs,NAC}}$ ratio against RCA content for different ranges of compressive strength and RCA water absorption, respectively. **As in Figure 1, the dashed lines connect the mean $\frac{\varepsilon_{cs,RAC}}{\varepsilon_{cs,NAC}}$ ratio within each RCA percentage.**

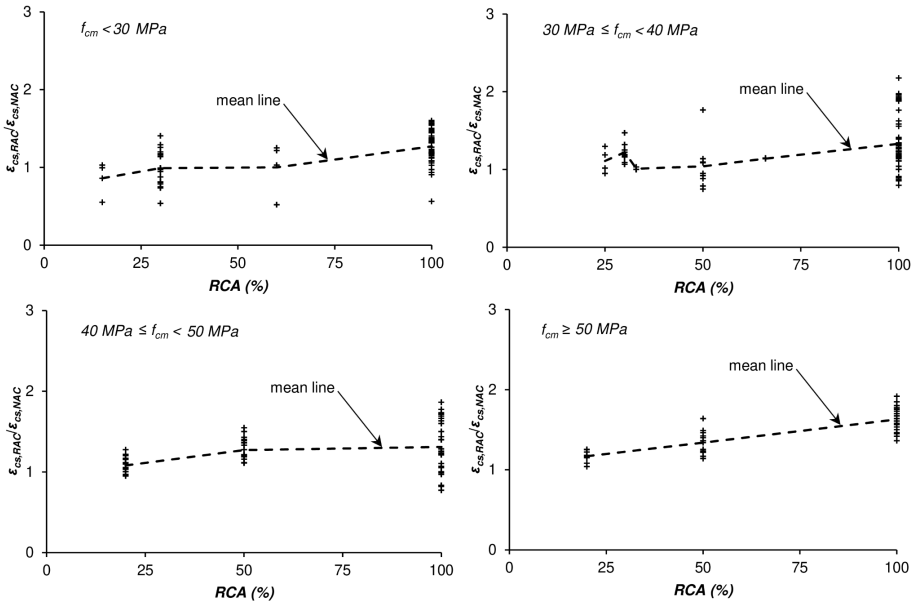

Fig. 3 $\frac{\varepsilon_{cs,RAC}}{\varepsilon_{cs,NAC}}$ ratio depending on RCA content and RAC compressive strength

From Figures 3 and 4 it can only be seen that, e.g., the scatter of $\frac{\varepsilon_{cs,RAC}}{\varepsilon_{cs,NAC}}$ within each RCA percentage tends to decrease with increasing compressive strength – it seems the variability becomes lower, perhaps because of the increasing stiffness and decreasing drying shrinkage of the cement paste itself, decreasing the importance of RCA stiffness. A relatively weak trend of increasing $\frac{\varepsilon_{cs,RAC}}{\varepsilon_{cs,NAC}}$ values with RCA percentage can be seen in all compressive strength ranges. As for the effect of water absorption, only a slight increasing trend with increasing RCA percentage is noticeable from the dashed lines connecting the mean values within RCA percentages.

3 Calculating RAC shrinkage strain using the *fib* Model Code 2010

3.1 *fib* Model Code 2010 performance on NAC

Since the second aim of this study was to test the applicability of the MC2010 shrinkage prediction model on RAC, it was first necessary to analyse the model itself and assess how the model performs on NAC. For this purpose, a much larger and more reliable database exists – the previously mentioned NU-ITI database [23].

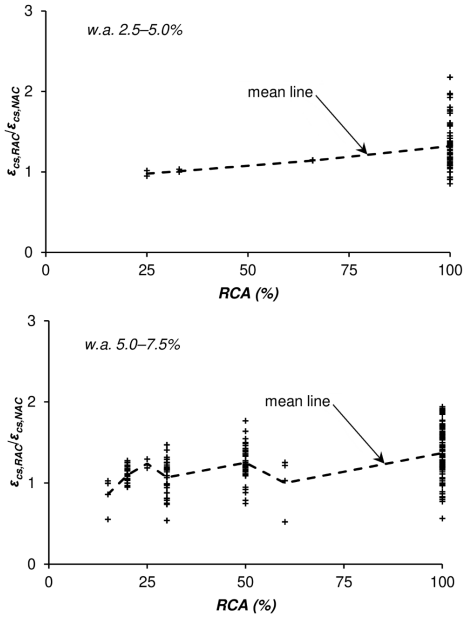

Fig. 4 $\frac{\varepsilon_{cs,RAC}}{\varepsilon_{cs,NAC}}$ ratio depending on RCA content and water absorption

MC2010 separates shrinkage strain ε_{cs} into a basic and drying component, ε_{cbs} and ε_{cds}, respectively:

$$\varepsilon_{cs}(t,t_s) = \varepsilon_{cbs}(t) + \varepsilon_{cds}(t,t_s) \tag{1}$$

where t is the current concrete age and t_s is the concrete age at the start of drying, in days.

Each of the two shrinkage components is defined as a product function of a 'final' shrinkage strain (dependent on parameters such as compressive strength, notional size and relative humidity) and a time development function. Basic (autogenous) shrinkage is modeled as

$$\varepsilon_{cbs}(t) = \varepsilon_{cbs0}(f_{cm}) \cdot \beta_{bs}(t) \tag{2}$$

and drying shrinkage as

$$\varepsilon_{cds}(t,t_s) = \varepsilon_{cds0}(f_{cm}) \cdot \beta_{RH} \cdot \beta_{ds}(t-t_s) \tag{3}$$

The final basic shrinkage strain is defined by

$$\varepsilon_{cbs0}(f_{cm}) = -\alpha_{bs}\left(\frac{f_{cm}/10}{6+f_{cm}/10}\right)^{2.5} \cdot 10^{-6} \tag{4}$$

and its time-development function by

$$\beta_{bs}(t) = 1 - exp(-0.2\sqrt{t}) \tag{5}$$

The final drying shrinkage strain is defined by

Table 3 Coefficients α_i [20]

Cement class	α_{bs}	α_{ds1}	α_{ds2}
32.5N	800	3	0.013
32.5R, 42.5N	700	4	0.012
42.5R, 52.5N, 52.5R	600	6	0.012

$$\varepsilon_{cds0}(f_{cm}) = [(220+110\alpha_{ds1})\cdot exp(-\alpha_{ds2}f_{cm})]\cdot 10^{-6} \tag{6}$$

the effect of relative humidity as

$$\beta_{RH} = \begin{cases} -1.55\left[1-\left(\frac{RH}{100}\right)^3\right] & \text{for } 40\% \le RH \le 99\% \cdot \beta_{s1} \\ 0.25 & \text{for } RH \ge 99\% \cdot \beta_{s1} \end{cases} \tag{7}$$

with

$$\beta_{s1} = \left(\frac{35}{f_{cm}}\right)^{0.1} \le 1.0 \tag{8}$$

The drying shrinkage time function is given as

$$\beta_{ds}(t-t_s) = \left(\frac{(t-t_s)}{0.035h_0^2+(t-t_s)}\right)^{0.5} \tag{9}$$

Finally, coefficients α_{bs}, α_{ds1}, and α_{ds2} are cement dependent and given in Table 3.

There are several existing studies testing the performance of the MC2010 model on NAC [24, 3, 1]. Hubler et al. [24] analysed the MC2010 model on the NU-ITI database (alongside models B3, B4, MC99, ACI209 and GL2000). The authors first tested individual predicted curves to test initial asymptotic and final parts of the shrinkage curve, thus varifying the mathematical form of the model's equations. After this, the authors also tested the overall performance of the model with fixed parameters on the NU-ITI database. When testing the quality of fit for individual curves, the CoV for MC2010 was 16.9% and 3.8% for the initial and final parts of the shrinkage curve, respectively; when testing its overall performance on the NU-ITI database, the CoV for residuals was 51% for the entire database and 40.8% for only concretes without admixtures.

For this study, an additional assessment of MC2010 was carried out on a 'filtered' version of the NU-ITI database. Starting from the database available in [23], criteria similar to the ones used for the RAC database described in section 2.1 were applied in order to obtain a larger database with similar ranges of parameters, enabling better comparison:

- only total shrinkage curves considered;
- compressive strength between 15 and 60 MPa;
- cement type specified;
- content of additives below 30% of cement amount;
- shrinkage specimen size specified; and
- relative humidity between 40 and 99%.

Again, only normal-strength concretes were considered with all information necessary for calculation of shrinkage according to MC2010 given. The lower limit on relative humidity was chosen according to MC2010 [20] and the upper limit was set in order not to consider swelling. Applying these criteria reduced the database from 1751 curves to 194 with 3423 data points. The range of compressive strengths in the new database was 16–59 MPa, 0.28–0.79 for *w/c* ratios, 30–273 mm for notional sizes, 40–84% for relative humidity, and 1–8960 days for time under drying $t - t_s$. Compared with the RAC database, the range of compressive strengths, *w/c* ratios and relative humidity are very similar, whereas here, notional sizes and time under drying cover a much larger range of values.

For each data point in the database, shrinkage strain was calculated according to the MC2010 model. Several statistical indicators were assessed in order to describe the model's performance. One way of assessing it is through a calculated-to-experimental shrinkage strain ratio, $\frac{\varepsilon_{cs,calc}}{\varepsilon_{cs,exp}}$. Then, a simple mean value and CoV for this ratio can be determined. In this case, a mean $\frac{\varepsilon_{cs,calc}}{\varepsilon_{cs,exp}}$ ratio of 1.042 is obtained with a CoV of 51%. The average performance of the model is excellent, but the scatter is very large. However, the traditional CoV does not take into account biases in the database such as large concentrations of values around shorter drying times. Hence, a better descriptor is one which gives equal importance to all drying times through weighting.

One such descriptor is the BP CoV, $\tilde{\omega_{BP}}$, developed by Bažant and Panula [5]. In this method, data points in each shrinkage curve (data set) (194 in this database) are divided into logarithmic time decades (0–9.9, 10–99.9, 100–999.9 days, etc.) and considered together. Then, weight coefficients are assigned to each point based on the decade it belongs to and on the number of data points in that decade. Finally, the overall CoV $\tilde{\omega_{BP}}$ is the root mean square of all the data set values [1].

$$\overline{O_j} = \frac{1}{n_w} \cdot \sum_{i=1}^{n} (\tilde{\omega_{ij}} \cdot O_{ij}) \tag{10}$$

$\overline{O_j}$ is the weighted average of the experimental (observed) shrinkage strain values, n_w is the sum of the weights of all data points in a data set (shrinkage curve), O_{ij} is the experimental shrinkage strain value for the i-th data point in data set j, and $\tilde{\omega_{ij}}$ is the weight assigned to the i-th data point in data set j:

$$\tilde{\omega_{ij}} = \frac{n_j}{n_d \cdot n_k} \tag{11}$$

where n_j in the number of data points in data set j, n_d is the number of logarithmic time decades spanned by measured data in set j, and n_k is the number of data points in the k-th decade. Then, the CoV for data set j is given by

$$\tilde{\omega_j} = \frac{1}{\overline{O_j}} \cdot \sqrt{\frac{1}{n-1} \cdot \sum_{i=1}^{n} \overline{\omega_{ij}} \cdot (C_{ij} - O_{ij})^2} \tag{12}$$

with C_{ij} being the calculated shrinkage strain value for the i-th data point in data set j. Finally, the overall BP CoV is determined using the total number of data sets N as

$$\tilde{\omega_{BP}} = \sqrt{\frac{1}{N} \cdot \sum_{j=1}^{N} \tilde{\omega_j}^2} \tag{13}$$

When calculated on this filtered NU-ITI database with 194 data sets, the BP CoV equals 19.9% which is a good result taking into account the intrinsic sources of variability associated with shrinkage. The database can be further improved by eliminating outlier $\frac{\varepsilon_{cs,calc}}{\varepsilon_{cs,exp}}$ ratios through a box-and-whiskers technique; this reduces the number of data points by only 54. The new mean $\frac{\varepsilon_{cs,calc}}{\varepsilon_{cs,exp}}$ ratio becomes 1.013 with a CoV of 47.5% and a BP CoV of 20.1%, i.e. the descriptors do not change significantly. The conclusion is that the MC2010 shrinkage model, on average, predicts the NAC shrinkage strain excellently, but with a significant scatter of the results. Nonetheless, it is still one of the best models available [24, 3, 1].

3.2 *fib* Model Code 2010 mathematical form verification for RAC

As explained in [24], any meaningful analysis of a shrinkage model must first consider the form of the shrinkage time development function, i.e. the ability of the model to qualitatively describe the evolution of shrinkage strain. Only then should databases be used to describe the global statistics of the model calibration.

In this first step, individual shrinkage curves were analysed and the model's free parameters were re-calibrated in order to minimise the CoV of the residuals, as given by Eq. 12. **In MC2010, the free parameters in the time evolution functions are coefficients -0.2 in Eq. 5 and 0.035 in Eq. 9 through which horizontal scaling of shrinkage curves can be achieved. Additionally, the overall basic and drying shrinkage strains in Eq. 1 can also be scaled; this is the case of vertical scaling.** As proposed by Project Team 1, currently working on the revision of Eurocode 2 [31], which uses the identical MC2010 shrinkage model, calibration can be done using equations 14, 15, and 16 and calibration coefficients $\xi_{cbs,1}$, $\xi_{cbs,2}$, $\xi_{cds,1}$, and $\xi_{cds,2}$:

$$\varepsilon_{cs}(t,t_s) = \xi_{cbs,1} \cdot \varepsilon_{cbs}(t) + \xi_{cds,1} \cdot \varepsilon_{cds}(t,t_s) \tag{14}$$

$$\beta_{bs}(t) = 1 - exp(-0.2 \cdot \xi_{cbs,2} \cdot \sqrt{t}) \tag{15}$$

$$\beta_{ds}(t-t_s) = \Big(\frac{(t-t_s)}{0.035 \cdot \xi_{cds,2} \cdot h_0^2 + (t-t_s)}\Big)^{0.5} \tag{16}$$

Shrinkage curves covering as many logarithmic time decades as possible should be used for this step. However, from the compiled RAC database, none of the shrinkage curves cover very early drying times, e.g. under one day. Hence, those curves with the longest drying times were selected for this analysis [32, 38]. Here, results will be shown for mixes 'NAC' and 'RAC' from [38] (RCA content 0% and 100% respectively) and mixes 'H50-0', 'H50-50' and 'H50-100' from [32] (RCA content 0%, 50%, and 100% respectively). The mixes cover a compressive strength range of 28–61 MPa, relative humidity 48–75%, notional size 60–75 mm and drying times 477–1000 days.

Varying the parameters $\xi_{cbs,1}$, $\xi_{cbs,2}$, $\xi_{cds,1}$, and $\xi_{cds,2}$ with the aim of reducing the weighted CoV of residuals (Eq. 12) led to results given in Figure 5. CoVs were obtained in the range of 2–3% for both NAC and RAC shrinkage curves. As can be seen in the figure, after re-fitting, MC2010 can describe equally well the time evolution of NAC and RAC shrinkage. **It should be noted that all five analysed shrinkage curves required both horizontal and vertical scaling, i.e. there were no systematic differences between RAC and NAC in this regard.**

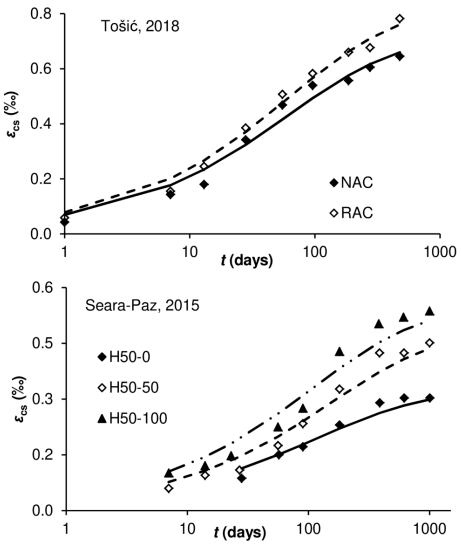

Fig. 5 Calibration of individual shrinkage curves from [32, 38]

The analysis in this section was used to demonstrate that the mathematical form of MC2010 is suitable for describing the time evolution of RAC shrinkage. In the following section, the analysis proceeds to assessing the overall calibration quality of the MC2010 model with its *default parameter values*. In other words, none of the calibration coefficients used in this section are used in the following analyses – parameters $\xi_{cbs,1}$, $\xi_{cbs,2}$, $\xi_{cds,1}$, and $\xi_{cds,2}$ are taken as equal to 1.

3.3 *fib* Model Code 2010 overall performance on RAC

The calculated shrinkage strain $\varepsilon_{cs,calc}$ was determined for the RAC database with previously eliminated outliers (as described in section 2.2) and using the MC2010 with default parameter values. The mean $\frac{\varepsilon_{cs,calc}}{\varepsilon_{cs,exp}}$ ratio and the BP CoV were chosen as statistical descriptors of the MC2010 model's performance, so that a comparison could be made with the results obtained on the filtered NU-ITI database from section 3.1. The results, classified according to RCA content, are given in Table 4. It should be noted that after eliminating outliers from the RAC database, in order to compute the BP CoV, four shrinkage curves were eliminated (three for 26–50% of RCA and one for 76–100% of RCA) which were left with only one data point and thus, the BP CoV could not be determined.

From the 'no RAC/NAC outliers' column in Table 4, it can be seen that for this particular sample of NAC shrinkage data, MC2010 significantly overestimates shrinkage with a mean $\frac{\varepsilon_{cs,calc}}{\varepsilon_{cs,exp}}$ ratio of 1.37 and a BP CoV of 35%. This stands in stark contrast to what was obtained on the filtered NU-ITI database in section 3.1 (mean of 1.013 and BP CoV of 20.1%). However, considering the scatter of the data in the NU-ITI database, obtaining such a 'sub-sample' as this one is not unlikely. One of potential reason for this could be ambient conditions which were not strictly controlled in many of the studies in the RAC database. Nonetheless, the comparison between RAC and companion NAC can be made. The second aspect to be highlighted from Table 4 is that for all RCA contents, except 76–100%, MC2010

Table 4 Statistical descriptors of the $\frac{\varepsilon_{cs,calc}}{\varepsilon_{cs,exp}}$ ratio

	No RAC/NAC outliers		No calc/exp outliers	
RCA %	μ	BP CoV (%)	μ	BP CoV (%)
0 (NAC)	1.37	35.0	1.28	28.7
1–25	1.54	45.2	1.54	45.2
26–50	1.40	35.1	1.39	40.6
51–75	1.33	15.8	1.33	15.8
76–100	0.96	19.3	0.92	19.3

overestimates shrinkage equally or even more than for NAC, with similar variability. However, for RAC with 76–100% of RCA (in this case, only 100%), it could be concluded that the model seems to predict shrinkage more precisely (mean ratio of 0.96 and a BP CoV of 19.3%). However, it should be kept in mind that a comparison of RAC and NAC shrinkage revealed a systematically higher shrinkage of RAC compared with companion NAC. Thus, this result seems logical.

The next step was to again eliminate outlier values, as in section 2.2, through a box-and-whiskers technique. This reduced the number of data points by 18 and the number of data sets by 2 (one NAC and one RAC 100%). The new statistical descriptors for the filtered database are given in Table 4 under the heading 'no calc/exp outliers'. The mean $\frac{\varepsilon_{cs,calc}}{\varepsilon_{cs,exp}}$ is now reduced to 1.28 for NAC, practically unchanged for RAC with 1–75% RCA and also reduced for RAC with 76–100% of RCA.

A scatter plot for this filtered NAC and RAC database, in the form of calculated vs. predicted values is given in Figure 6. The black full lines represent mean lines, the gray full lines represent the equality line and the black dashed lines represent 5 and 95 percentile lines for the data. For NAC, the systematic overestimation can be seen. For RAC, the model behaviour seems more symmetric but with a larger scatter. Moreover, the majority of overestimated values are for RCA contents below 75%, whereas the majority of underestimated ones are for RCA contents above 75%. For both samples, a relatively weak but similar coefficient of determination (R^2) was found as indicated in Figure 6.

If only the results for RAC were analysed, it could be concluded that MC2010 behaves very well, slightly underestimating RAC shrinkage. However, since section 2.2 revealed that relative to a companion NAC, RAC shrinkage is significantly larger, this cannot be ignored and seems to point to an actual underestimation of RAC shrinkage by the MC2010 model (since for companion NAC, the mean $\frac{\varepsilon_{cs,calc}}{\varepsilon_{cs,exp}}$ ratio is 1.28). One possibility is that, although the database contains RAC and *companion* NAC, the companion NAC actually have larger strengths, thus explaining the difference in shrinkage and the performance of MC2010. If this were the case, then it could be claimed that MC2010 predicts RAC shrinkage appropriate to its compressive strength. However, when the database is analysed, it is revealed that the difference in compressive strengths is only 7% on average (the mean RAC-NAC strength ratio is 0.93) with a CoV of 12.9%. This difference is insufficient to explain the gap in shrinkage values. Since MC2010 uses as input only compressive strength (beside cement type which is identical between RAC and companion NAC), replacing RAC compressive strength with that of its companion NAC should lead to equal predicted shrinkage strains. However, doing this changes the mean $\frac{\varepsilon_{cs,calc}}{\varepsilon_{cs,exp}}$ ratio insignificantly, e.g. for RAC with 100% RCA (for which differences in f_{cm} are largest) the new $\frac{\varepsilon_{cs,calc}}{\varepsilon_{cs,exp}}$ ratio becomes 0.91 instead of 0.92.

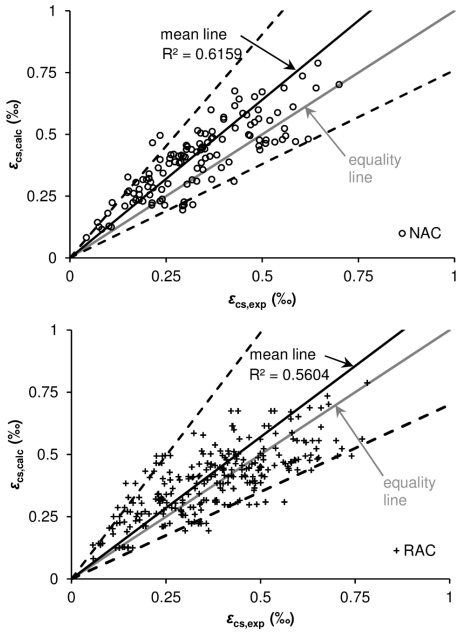

Fig. 6 Calculated vs. experimental shrinkage strain values for NAC and RAC with eliminated outlier values

This is an unambiguous conclusion that MC2010 systematically underestimates the shrinkage of RAC and needs to be corrected to take into account its specifics. Any correction done on this database should lead to equal performance as on companion NAC, i.e. a mean $\frac{\varepsilon_{cs,calc}}{\varepsilon_{cs,exp}}$ ratio of 1.28. **As shown in the discussion in section 2.2, there is only a need for vertical scaling of RAC shrinkage magnitude. Any need for horizontal scaling of RAC shrinkage time evolution could not be identified on this database.**

4 RAC shrinkage strain correction coefficient for the *fib* Model Code 2010

The final aim of this study was to formulate a correction coefficient for RAC shrinkage strain to be used in conjunction with MC2010. Since the studies in the RAC database do not separate RAC shrinkage into basic and drying, it was only possible to formulate a *global* correction coefficient $\xi_{cs,RAC}$ in the following form:

$$\varepsilon_{cs,RAC} = \xi_{cs,RAC} \cdot \varepsilon_{cs,calc} \tag{17}$$

where $\varepsilon_{cs,calc}$ is the shrinkage strain calculated according to MC2010 (as for any NAC) using Eqs. 1 to 9. This is similar in principle to the correction coefficient proposed in [28], however, here, an analytic expression will be given. **The proposed coefficient is a vertical scaling factor and the adopted approach in Eq. 17 amounts to adopting correction factors $\xi_{cbs,1}$ and $\xi_{cds,1}$ in Eq. 14 as equal. In other words, basic and drying shrinkage components will be equally vertically scaled. Since there are insufficient data for separate analyses of both shrinkage components, such an approach is justified, even though it leads to potentially non-unique solutions ($\varepsilon_{cs,RAC}$ in Eq. 17 obtained using $\xi_{cs,RAC}$ can also be obtained using Eq. 14 and multiple combinations of factors $\xi_{cbs,1}$ and $\xi_{cds,1}$).**

As stated earlier, three potential parameters were identified influencing the relative increase in RAC shrinkage: RAC compressive strength, f_{cm} (in MPa), RCA content, RCA% (in %), and RCA water absorption, *w.a.* (in %). Since the statistical comparisons of RAC and companion NAC in this study constituted a purely empirical approach, the optimal form for the correction coefficient $\xi_{cs,RAC}$ was chosen as a multivariate power function. The general form for the correction coefficient is proposed as

$$\xi_{cs,RAC} = x_1 \cdot (f_{cm})^{x_2} \cdot (RCA\%)^{x_3} \cdot (w.a.)^{x_4} \tag{18}$$

The calibration procedure was as follows. Since the aim was to bring MC2010's performance on RAC to the same level of companion NAC, it was necessary to increase the $\frac{\varepsilon_{cs,calc}}{\varepsilon_{cs,exp}}$ ratio to 1.28 for all RCA contents. First, for each RAC shrinkage curve, after calculating shrinkage strain using MC2010, a unique value for $\xi_{cs,RAC}$ was calibrated for that curve to bring the $\frac{\varepsilon_{cs,calc}}{\varepsilon_{cs,exp}}$ ratio to 1.28. This led to 81 unique calibrated $\xi_{cs,RAC}$ values (the remaining number of RAC shrinkage curves).

Then, the coefficients in Eq. 18 were fitted in order to match as closely as possible the values of the $\xi_{cs,RAC}$ coefficient determined for each shrinkage curve individually. As a first results, $\xi_{cs,RAC}$ was obtained as

$$\xi_{cs,RAC} = 2.615 \cdot (f_{cm})^{-0.15} \cdot (RCA\%)^{0.15} \cdot (w.a.)^{-0.50} \tag{19}$$

Using Eq. 19, the mean calculated-to-manually calibrated ratio for $\xi_{cs,RAC}$ is 1.035 with a CoV of 22.2%. Generally, this is a good result, considering the scatter in the database. **However, since RCA water absorption is usually not known in the design stage, its elimination from Eq. 19 would produce a simpler and more practical version of the $\xi_{cs,RAC}$ coefficient. Adopting x_4 = 0 and repeating the analysis led to the following expression for $\xi_{cs,RAC}$:**

$$\xi_{cs,RAC} = 1.0 \cdot (f_{cm})^{-0.3} \cdot (RCA\%)^{0.3} \tag{20}$$

Equation 20 has a very simple form and its predictive ability is even slightly improved compared with Eq. 19: the mean calculated-to-manually calibrated ratio for $\xi_{cs,RAC}$ is 1.01 with a CoV of 21.6%. This proves the possibility of eliminating RCA water absorption as a model parameter while preserving the model's predictive ability.

The correction coefficient $\xi_{cs,RAC}$ was calibrated considering also values smaller than 1.0, i.e. cases where RAC had lower shrinkage than companion NAC. However, as the final version of the coefficient, to be used in conjunction with the MC2010 shrinkage model, a lower limit of 1.0 was imposed. Finally, $\xi_{cs,RAC}$ should be calculated as

$$\xi_{cs,RAC} = \left(\frac{RCA\%}{f_{cm}}\right)^{0.3} \geq 1.0 \tag{21}$$

In Eq. 21, f_{cm} should be input in MPa and *RCA%* in %.

As an illustration, the correction coefficient is plotted against RCA content, for various RAC compressive strengths, in Figure 7 to demonstrate its dependence on both parameters in Eq. 21. It can be seen to increase with increasing RCA content and decreasing compressive strength, describing the general conclusion of previous sections. An interesting aspect of Eq. 21 is that, because of the same exponent for f_{cm} and RCA%, $\xi_{cs,RAC}$ is equal to 1.0 as long as compressive strength is greater than the RCA replacement ratio. For example, $\xi_{cs,RAC}$ becomes greater than 1.0 if f_{cm} = 50 MPa, only for RCA content above 50%, Figure 7. For illustration, for RAC with 100% RCA and f_{cm} 30–40 MPa, the most usual range in

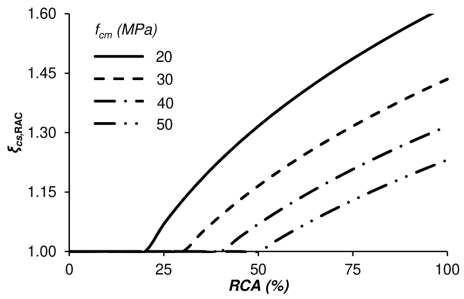

Fig. 7 Correction coefficient $\xi_{cs,RAC}$ for different compressive strengths and RCA contents

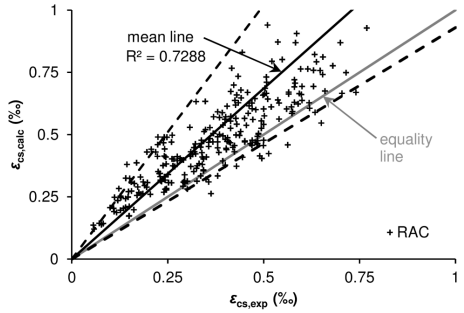

Fig. 8 Calculated vs. experimental shrinkage strain values for RAC using the $\xi_{cs,RAC}$ coefficient

the database, $\xi_{cs,RAC}$ is 1.44–1.32, precisely around the observed mean $\frac{\varepsilon_{cs,RAC}}{\varepsilon_{cs,NAC}}$ ratio in Table 1.

Figure 8 presents a scatter plot of calculated-to-experimentally measured RAC shrinkage strain, similar to Fig. 6 but calculated using the $\xi_{cs,RAC}$ coefficient from Eq. 21. Compared with Fig. 6, a shift towards higher $\frac{\varepsilon_{cs,calc}}{\varepsilon_{cs,exp}}$ ratios can be seen, similar to the results for NAC in Fig. 6, as was intended. Additionally, the coefficient of determination R^2 is increased from 0.56 to 0.73 which is a significant result.

Another useful point about the $\xi_{cs,RAC}$ coefficient in its form in Eq. 18 and the freely available database given as Online Resource 1, is the fact that it can easily be updated in the future – new studies and results can be added and new parameter optimizations for $\xi_{cs,RAC}$ can be performed.

Everything said in section 5.1.9.4.4 of the *fib* Model Code 2010 about analysing shrinkage effects in reinforced NAC structures [20], holds for RAC as well. Because of its similar scatter, more detailed analysis should include taking the 10 and 5% cut-off values of the shrinkage strain, assuming a normal distribution. However, with this approach, the cut-off value needs to be formed from the shrinkage strain $\varepsilon_{cs,RAC}$ as given by Eq. 17. As in the case of NAC structures, if the design with these cut-off values does not provide satisfactory results, tests and calibrations of the model, according to Eq. 14, 15, and 16 should be performed.

5 Conclusions

This paper described a meta-analysis of previously published studies on the shrinkage strain of RAC through the formation of a database of experimental results on RAC and companion NAC shrinkage strain. Using statistical analyses, a comparison was made between predictions obtained using the *fib* Model Code 2010 for RAC and companion NAC shrinkage strain. Taking into account the large scatter of experimental results, which introduces significant uncertainties into shrinkage strain predictions using existing models (including the *fib* Model Code 2010 model), the following conclusions are drawn:

1. From the extensive list of previously published research on RAC shrinkage, only a smaller number of studies provide all necessary information for meaningful comparisons and analyses. In this study, 19 studies with 125 shrinkage curves (39 NAC and 86 RAC) and 424 data points entered into the database, freely available as Online Resource 1;
2. Compared with larger databases for NAC shrinkage, such as the NU-ITI database, the experiments on RAC shrinkage are characterized with a lower range of compressive strengths, poorer control of ambient conditions during testing and a much shorter average and maximum test duration;
3. A comparison of RAC and NAC experimental shrinkage strain, $\frac{\varepsilon_{cs,RAC}}{\varepsilon_{cs,NAC}}$, revealed that on average RAC has a higher shrinkage strain compared with a companion NAC concrete (having an identical *w/c* ratio). Although the scatter in the database is very large, this difference can generally be said to increase with increasing RCA content and decreasing compressive strength. For RAC with 100% of RCA the average increase in total shrinkage strain is 35% relative to companion NAC;
4. **The difference between RAC and companion NAC shrinkage is in shrinkage magnitude, i.e. RAC shrinkage curves are vertically scaled compared with companion NAC shrinkage curves. The current database did not reveal different time evolution of RCA shrinkage compared with companion NAC, i.e. RAC shrinkage curves do not seem to be horizontally scaled compared with companion NAC shrinkage curves. This is potentially due to counteracting effects of higher porosity and lower stiffness of RCA and its internal curing effect on RAC. Nonetheless, more experiments separating RAC shrinkage into basic and drying components are necessary**;
5. Applying the *fib* Model Code 2010 shrinkage model by fitting to individual RAC shrinkage curves revealed that the model's mathematical form enables the accurate description of the time evolution of RAC shrinkage strain. However, applying the MC2010 model with its default parameter values on the RAC database showed its underestimation of RAC shrinkage strain;
6. A correction coefficient $\xi_{cs,RAC}$ for the RAC shrinkage strain was formulated as a bivariate power function with RAC compressive strength and RCA content as variables. The correction coefficient should be used to multiply the shrinkage strain $\varepsilon_{cs,calc}$ calculated according to MC2010. The correction coefficient is practical for use since the required inputs are available in the design stage;

All of the stated conclusions depend highly upon the database from which they were drawn and are only valid in the current range of parameter values. However, making the database freely available makes it easy for the research community to update it, improve it, and analyse it in ways different from the one presented in this study.

Funding This work was supported by the Ministry for Education, Science and Technology, Republic of Serbia [grant number TR36017] and the SAES project [BIA2016-78742-C2-1-R] of the Spanish Ministerio de Economía, Industria y Competitividad. This support is gratefully acknowledged.

Compliance with ethical standards

Conflict of interest The authors declare that they have no conflict of interest.

References

1. ACI 2092R-08 (2008) Guide for Modeling and Calculating Shrinkage and Creep in Hardened Concrete. American Concrete Institute, Farmington Hills, MI
2. ACI 209R-92 (1992) Prediction of Creep, Shrinkage, and Temperature Effects in Concrete Structures. American Concrete Institute, Farmington Hills, MI
3. Al-Manaseer A, Prado A (2015) Statistical Comparisons of Creep and Shrinkage Prediction Models Using RILEM and NU-ITI Databases. ACI Materials Journal 112(1):125–135
4. Amorim P, De Brito J, Evangelista L (2012) Concrete made with coarse concrete aggregate: Influence of curing on durability. ACI Materials Journal 109(2):195–204, DOI 10.14359/51683706
5. Bažant Z, Panula L (1978) Practical prediction of time-dependent deformations of concrete. Part I: Shrinkage. Part II: Basic creep. Part III: Drying creep. Part IV: Temperature effect on basic creep. Materials and Structures 11:307–434
6. Bažant Z, Hauggaard AB, Baweja S, Ulm Fj (1997) Microprestress-solidification theory for concrete creep. I: Aging and drying effects. Journal of Engineering Mechanics 123(11):1188–1194, DOI 10.1061/(ASCE)0733-9399(1997)123:11(1188)
7. Bažant Z, Hubler M, Wendner R (2015) RILEM draft recommendation: TC-242-MDC multi-decade creep and shrinkage of concrete: material model and structural analysis. Materials and Structures 48:753–770, DOI 10.1617/s11527-014-0485-2
8. Beltrán MG, Barbudo A, Agrela F, Galvín AP, Jiménez JR (2014) Effect of cement addition on the properties of recycled concretes to reach control concretes strengths. Journal of Cleaner Production 79:124–133, DOI 10.1016/j.jclepro.2014.05.053
9. Brand AS, Roesler JR, Salas A (2015) Initial moisture and mixing effects on higher quality recycled coarse aggregate concrete. Construction and Building Materials 79:83–89, DOI 10.1016/j.conbuildmat.2015.01.047
10. Castaño JO, Domingo A, Lazaro C (2009) A study on drying shrinkage and creep of recycled concrete aggregate. In: Proceedings of the International Association for Shell and Spatial Structures (IASS) Symposium 2009, pp 2955–2964
11. CEB-FIP (1978) Model Code 1978. Comite Euro-International Du Beton, Paris
12. CEB-FIP (1991) Model Code 1990. Comite Euro-International Du Beton, Paris, DOI 10.1680/ceb-fipmc1990.35430
13. Corinaldesi V (2010) Mechanical and elastic behaviour of concretes made of recycled-concrete coarse aggregates. Construction and Building Materials 24(9):1616–1620, DOI 10.1016/j.conbuildmat.2010.02.031
14. Corinaldesi V, Moriconi G (2010) Recycling of rubble from building demolition for low-shrinkage concretes. Waste Management 30(4):655–659, DOI 10.1016/j.wasman.2009.11.026

15. Domingo A, Lázaro C, Gayarre FL, Serrano MA, López-Colina C (2010) Long term deformations by creep and shrinkage in recycled aggregate concrete. Materials and Structures 43(8):1147–1160, DOI 10.1617/s11527-009-9573-0
16. Duan ZH, Poon CS (2014) Properties of recycled aggregate concrete made with recycled aggregates with different amounts of old adhered mortars. Materials and Design 58:19–29, DOI 10.1016/j.matdes.2014.01.044
17. EN 1992-1-1 (2004) Eurocode 2: Design of concrete structures - Part 1-1: General rules and rules for buildings. CEN, Brussels
18. Fan Y, Xiao J, Tam VW (2014) Effect of old attached mortar on the creep of recycled aggregate concrete. Structural Concrete 15(2):169–178
19. Fathifazl G, Razaqpur G (2013) Creep rheological models for recycled aggregate concrete. ACI Materials Journal 2(110):115–125
20. FIB (2013) fib Model Code for Concrete Structures 2010. International Federation for Structural Concrete (fib), Lausanne, DOI 10.1002/9783433604090, arXiv:1011.1669v3
21. Gómez-Soberón JM (2002) Shrinkage of concrete with replacement of aggregate with recycled concrete aggregate. ACI Special Publications 209:475–496
22. Ho N, Lee Y, Lim W, Zayed T, Chew K, Low G, Ting S (2013) Efficient utilization of recycled concrete aggregate in structural concrete. Journal of Materials in Civil Engineering 25(3):318–327, DOI 10.1061/(ASCE)MT.1943-5533
23. Hubler MH, Wendner R, Bažant Z (2015) Comprehensive Database for Concrete Creep and Shrinkage: Analysis and Recommendations for Testing and Recording. ACI Materials Journal 112(4):547–558, DOI 10.14359/51687453, URL http://www.concrete.org/Publications/InternationalConcreteAbstractsPortal.aspx?m=details&i=51687453
24. Hubler MH, Wendner R, Bažant Z (2015) Statistical justification of Model B4 for drying and autogenous shrinkage of concrete and comparisons to other models. Materials and Structures 48:797–814, DOI 10.1617/s11527-014-0516-z
25. Ignjatović I (2013) Ultimate strength of reinforced recycled concrete beams. Doctoral dissertation, University of Belgrade
26. Kou Sc, Poon Cs (2015) Effect of the quality of parent concrete on the properties of high performance recycled aggregate concrete. Construction and Building Materials 77:501–508, DOI 10.1016/j.conbuildmat.2014.12.035
27. Le Chatelier H (1887) Experimental researches on the constitution of hydraulic mortars. McGraw Publishing Company, New York
28. Lye Cq, Ghataora GS, Dhir RK (2016) Shrinkage of recycled aggregate concrete. In: Structures and Buildings, Proceedings of the Institution of Civil Engineers, ICE, pp 1–25, DOI 10.1680/jstbu.15.00138
29. Neville A (1995) Properties of concrete. Pearson Education Ltd, Harlow
30. Pedro D, de Brito J, Evangelista L (2014) Performance of concrete made with aggregates recycled from precasting industry waste: influence of the crushing process. Materials and Structures/Materiaux et Constructions 48(12):3965–3978, DOI 10.1617/s11527-014-0456-7
31. PT1prEN1992-1-1 (2017) Eurocode 2: Design of concrete structures – Part 1-1: General rules, rules for buildings, bridges and civil engineering structures. CEN, Brussels
32. Seara-Paz S (2015) Efect of long-term deformations in structural flexural performance and bond behaviour analysis of recycled concrete. Phd, Universidade de Coruna
33. Shaikh F, Nguyen H (2013) Properties of concrete containing recycled construction and demolition wastes as coarse aggregates. Journal of Sustainable Cement-Based Materials 2:204–217

34. Silva R (2015) Use of recycled aggregates from construction and demolition waste in the production of structural concrete. Doctoral dissertation, Universidade de Lisboa
35. Soares D, De Brito J, Ferreira J, Pacheco J (2014) Use of coarse recycled aggregates from precast concrete rejects: Mechanical and durability performance. Construction and Building Materials 71:263–272, DOI 10.1016/j.conbuildmat.2014.08.034
36. Sri Ravindrarajah R, Tam CT (1985) Properties of concrete made with crushed concrete as coarse aggregate. Magazine of Concrete Research 37(130):29–38, DOI 10.1680/macr.1985.37.130.29
37. Tazawa Ei (1999) Autogenous shrinkage of concrete. E & FN Spon, London
38. Tošić N (2018) Behaviour of reinforced concrete beams made with recycled and waste materials under long-term loading. Doctoral dissertation, University of Belgrade
39. Yang KH, Chung HS, Ashour AF (2008) Influence of type and replacement level of recycled aggregates on concrete properties. ACI Materials Journal 105(3):289–296, DOI 10.14359/19826

Article Title: *Shrinkage of recycled aggregate concrete: experimental database and application of Model C*

Journal: *Materials and Structures*

Authors: *Nikola Tošić* [1]

Albert de la Fuente [2]

Snežana Marinković [1]

Affiliations: [1] *University of Belgrade, Faculty of Civil Engineering, Bulevar kralja Aleksandra 73, 11000 Be*

[2] *Civil and Environmental Engineering Department, Universitat Politécnica de Catalunya (UPC*

E-mail: ntosic@imk.grf.bg.ac.rs

ode 2010

lgrade, Serbia
), Jordi Girona 1–3, 08034 Barcelona, Spain

172

	Ref	Data	Mix	Coarse RCA %
1	*1*	*Figure*	*C1-0*	*0*
2	*1*	*Figure*	*C1-0*	*0*
3	*1*	*Figure*	*C1-0*	*0*
4	*1*	*Figure*	*C1-20*	*20*
5	*1*	*Figure*	*C1-20*	*20*
6	*1*	*Figure*	*C1-20*	*20*
7	*1*	*Figure*	*C1-50*	*50*
8	*1*	*Figure*	*C1-50*	*50*
9	*1*	*Figure*	*C1-50*	*50*
10	*1*	*Figure*	*C1-100*	*100*
11	*1*	*Figure*	*C1-100*	*100*
12	*1*	*Figure*	*C1-100*	*100*
13	*1*	*Figure*	*C2-0*	*0*
14	*1*	*Figure*	*C2-0*	*0*
15	*1*	*Figure*	*C2-0*	*0*
16	*1*	*Figure*	*C2-20*	*20*
17	*1*	*Figure*	*C2-20*	*20*
18	*1*	*Figure*	*C2-20*	*20*
19	*1*	*Figure*	*C2-50*	*50*
20	*1*	*Figure*	*C2-50*	*50*
21	*1*	*Figure*	*C2-50*	*50*
22	*1*	*Figure*	*C2-100*	*100*
23	*1*	*Figure*	*C2-100*	*100*
24	*1*	*Figure*	*C2-100*	*100*
49	*3*	*Figure*	*NAC 0.5*	*0*
50	*3*	*Figure*	*NAC 0.5*	*0*
51	*3*	*Figure*	*NAC 0.5*	*0*
52	*3*	*Figure*	*RAC20 0.5*	*20*
53	*3*	*Figure*	*RAC20 0.5*	*20*
54	*3*	*Figure*	*RAC20 0.5*	*20*
55	*3*	*Figure*	*RAC50 0.5*	*50*
56	*3*	*Figure*	*RAC50 0.5*	*50*
57	*3*	*Figure*	*RAC50 0.5*	*50*
58	*3*	*Figure*	*RAC100 0.5*	*100*
59	*3*	*Figure*	*RAC100 0.5*	*100*
60	*3*	*Figure*	*RAC100 0.5*	*100*
61	*3*	*Figure*	*NAC 0.65*	*0*
62	*3*	*Figure*	*NAC 0.65*	*0*
63	*3*	*Figure*	*NAC 0.65*	*0*
64	*3*	*Figure*	*RAC20 0.65*	*20*
65	*3*	*Figure*	*RAC20 0.65*	*20*
66	*3*	*Figure*	*RAC20 0.65*	*20*
67	*3*	*Figure*	*RAC50 0.65*	*50*
68	*3*	*Figure*	*RAC50 0.65*	*50*
69	*3*	*Figure*	*RAC50 0.65*	*50*
70	*3*	*Figure*	*RAC100 0.65*	*100*
71	*3*	*Figure*	*RAC100 0.65*	*100*
72	*3*	*Figure*	*RAC100 0.65*	*100*
245	*10*	*Figure*	*RC*	*0*
246	*10*	*Figure*	*RC*	*0*
247	*10*	*Figure*	*RC*	*0*
248	*10*	*Figure*	*RC*	*0*

249	*10*	*Figure*	*C20*	*20*
250	*10*	*Figure*	*C20*	*20*
251	*10*	*Figure*	*C20*	*20*
252	*10*	*Figure*	*C20*	*20*
253	*10*	*Figure*	*C50*	*50*
254	*10*	*Figure*	*C50*	*50*
255	*10*	*Figure*	*C50*	*50*
256	*10*	*Figure*	*C50*	*50*
257	*10*	*Figure*	*C100*	*100*
258	*10*	*Figure*	*C100*	*100*
259	*10*	*Figure*	*C100*	*100*
260	*10*	*Figure*	*C100*	*100*
261	*11*	*Figure*	*NAT+SP*	*0*
262	*11*	*Figure*	*NAT+SP*	*0*
263	*11*	*Figure*	*NAT+SP*	*0*
264	*11*	*Figure*	*NAT+SP+SRA*	*0*
265	*11*	*Figure*	*NAT+SP+SRA*	*0*
266	*11*	*Figure*	*NAT+SP+SRA*	*0*
267	*11*	*Figure*	*RECSAT+SP*	*50*
268	*11*	*Figure*	*RECSAT+SP*	*50*
269	*11*	*Figure*	*RECSAT+SP*	*50*
270	*11*	*Figure*	*RECSAT+SP+SRA*	*50*
271	*11*	*Figure*	*RECSAT+SP+SRA*	*50*
272	*11*	*Figure*	*RECSAT+SP+SRA*	*50*
273	*11*	*Figure*	*REC+SP*	*50*
274	*11*	*Figure*	*REC+SP*	*50*
275	*11*	*Figure*	*REC+SP*	*50*
276	*11*	*Figure*	*REC+SP+SRA*	*50*
277	*11*	*Figure*	*REC+SP+SRA*	*50*
278	*11*	*Figure*	*REC+SP+SRA*	*50*
279	*12*	*Figure*	*H40-A 0*	*0*
280	*12*	*Figure*	*H40-A 0*	*0*
281	*12*	*Figure*	*H40-A 0*	*0*
282	*12*	*Figure*	*H40-A 0*	*0*
283	*12*	*Figure*	*H40-A 0*	*0*
284	*12*	*Figure*	*H40-A 0*	*0*
285	*12*	*Figure*	*H40-A 20*	*20*
286	*12*	*Figure*	*H40-A 20*	*20*
287	*12*	*Figure*	*H40-A 20*	*20*
288	*12*	*Figure*	*H40-A 20*	*20*
289	*12*	*Figure*	*H40-A 20*	*20*
290	*12*	*Figure*	*H40-A 20*	*20*
291	*12*	*Figure*	*H40-A 50*	*50*
292	*12*	*Figure*	*H40-A 50*	*50*
293	*12*	*Figure*	*H40-A 50*	*50*
294	*12*	*Figure*	*H40-A 50*	*50*
295	*12*	*Figure*	*H40-A 50*	*50*
296	*12*	*Figure*	*H40-A 50*	*50*
297	*12*	*Figure*	*H40-A 100*	*100*
298	*12*	*Figure*	*H40-A 100*	*100*
299	*12*	*Figure*	*H40-A 100*	*100*
300	*12*	*Figure*	*H40-A 100*	*100*
301	*12*	*Figure*	*H40-A 100*	*100*
302	*12*	*Figure*	*H40-A 100*	*100*
303	*13*	*Figure*	*NAC*	*0*

304	*13*	*Figure*	*NAC*	*0*
305	*13*	*Figure*	*NAC*	*0*
306	*13*	*Figure*	*RAC33*	*33*
307	*13*	*Figure*	*RAC33*	*33*
308	*13*	*Figure*	*RAC33*	*33*
309	*13*	*Figure*	*RAC66*	*66*
310	*13*	*Figure*	*RAC66*	*66*
311	*13*	*Figure*	*RAC66*	*66*
312	*13*	*Figure*	*RAC100*	*100*
313	*13*	*Figure*	*RAC100*	*100*
314	*13*	*Figure*	*RAC100*	*100*
315	*14*	*Figure*	*NA-I*	*0*
316	*14*	*Figure*	*NA-I*	*0*
317	*14*	*Figure*	*RA30-I*	*100*
318	*14*	*Figure*	*RA30-I*	*100*
319	*14*	*Figure*	*RA45-I*	*100*
320	*14*	*Figure*	*RA45-I*	*100*
321	*14*	*Figure*	*RA60-I*	*100*
322	*14*	*Figure*	*RA60-I*	*100*
323	*14*	*Figure*	*RA80-I*	*100*
324	*14*	*Figure*	*RA80-I*	*100*
325	*14*	*Figure*	*RA100-I*	*100*
326	*14*	*Figure*	*RA100-I*	*100*
327	*15*	*Figure*	*RC45PC*	*0*
328	*15*	*Figure*	*RC45PC*	*0*
329	*15*	*Figure*	*C100L45PC*	*100*
330	*15*	*Figure*	*C100L45PC*	*100*
331	*15*	*Figure*	*C100P45PC*	*100*
332	*15*	*Figure*	*C100P45PC*	*100*
333	*15*	*Figure*	*RC45PSC*	*0*
334	*15*	*Figure*	*RC45PSC*	*0*
335	*15*	*Figure*	*C100L45PSC*	*100*
336	*15*	*Figure*	*C100L45PSC*	*100*
337	*15*	*Figure*	*C100P45PSC*	*100*
338	*15*	*Figure*	*C100P45PSC*	*100*
339	*15*	*Figure*	*RC65PC*	*0*
340	*15*	*Figure*	*RC65PC*	*0*
341	*15*	*Figure*	*C100L65PC*	*100*
342	*15*	*Figure*	*C100L65PC*	*100*
343	*15*	*Figure*	*C100P65PC*	*100*
344	*15*	*Figure*	*C100P65PC*	*100*
345	*15*	*Figure*	*RC65PSC*	*0*
346	*15*	*Figure*	*RC65PSC*	*0*
347	*15*	*Figure*	*C100L65PSC*	*100*
348	*15*	*Figure*	*C100L65PSC*	*100*
349	*15*	*Figure*	*C100P65PSC*	*100*
350	*15*	*Figure*	*C100P65PSC*	*100*
351	*16*	*Figure*	*1*	*0*
352	*16*	*Figure*	*1*	*0*
353	*16*	*Figure*	*2*	*25*
354	*16*	*Figure*	*2*	*25*
355	*16*	*Figure*	*3*	*50*
356	*16*	*Figure*	*3*	*50*
357	*17*	*Figure*	*RC*	*0*
358	*17*	*Figure*	*RC*	*0*

359	*17*	*Figure*	*C25*	*25*
360	*17*	*Figure*	*C25*	*25*
361	*17*	*Figure*	*C100*	*100*
362	*17*	*Figure*	*C100*	*100*
363	*18*	*Figure*	*Control mix*	*0*
364	*18*	*Figure*	*Control mix*	*0*
365	*18*	*Figure*	*RGI-100*	*100*
366	*18*	*Figure*	*RGI-100*	*100*
367	*18*	*Figure*	*RGIII-100*	*100*
368	*18*	*Figure*	*RGIII-100*	*100*

RCA source and composition	Water absorption (%)[1]
n/a	1.53
n/a	1.53
n/a	1.53
Old blocks and mortar from recycling plant (>85% crushed concrete)	6.94
Old blocks and mortar from recycling plant (>85% crushed concrete)	6.94
Old blocks and mortar from recycling plant (>85% crushed concrete)	6.94
Old blocks and mortar from recycling plant (>85% crushed concrete)	6.94
Old blocks and mortar from recycling plant (>85% crushed concrete)	6.94
Old blocks and mortar from recycling plant (>85% crushed concrete)	6.94
Old blocks and mortar from recycling plant (>85% crushed concrete)	6.94
Old blocks and mortar from recycling plant (>85% crushed concrete)	6.94
Old blocks and mortar from recycling plant (>85% crushed concrete)	6.94
n/a	1.53
n/a	1.53
n/a	1.53
Old blocks and mortar from recycling plant (>85% crushed concrete)	6.94
Old blocks and mortar from recycling plant (>85% crushed concrete)	6.94
Old blocks and mortar from recycling plant (>85% crushed concrete)	6.94
Old blocks and mortar from recycling plant (>85% crushed concrete)	6.94
Old blocks and mortar from recycling plant (>85% crushed concrete)	6.94
Old blocks and mortar from recycling plant (>85% crushed concrete)	6.94
Old blocks and mortar from recycling plant (>85% crushed concrete)	6.94
Old blocks and mortar from recycling plant (>85% crushed concrete)	6.94
Old blocks and mortar from recycling plant (>85% crushed concrete)	6.94
n/a	1.20
n/a	1.20
n/a	1.20
No data	5.19
No data	5.19
No data	5.19
No data	5.19
No data	5.19
No data	5.19
No data	5.19
No data	5.19
No data	5.19
n/a	1.20
n/a	1.20
n/a	1.20
No data	5.19
No data	5.19
No data	5.19
No data	5.19
No data	5.19
No data	5.19
No data	5.19
No data	5.19
No data	5.19
n/a	1.30
n/a	1.30
n/a	1.30
n/a	1.30

Unclear/No data	*6.10*
Unclear/No data	*6.10*
Unclear/No data	*6.10*
Unclear/No data	*6.10*
Unclear/No data	*6.10*
Unclear/No data	*6.10*
Unclear/No data	*6.10*
Unclear/No data	*6.10*
Unclear/No data	*6.10*
Unclear/No data	*6.10*
Unclear/No data	*6.10*
n/a	*1.80*
n/a	*1.80*
n/a	*1.80*
n/a	*1.80*
n/a	*1.80*
n/a	*1.80*
Demolition waste from a plant (83% concrete, 13% masonry, 3% other)	*7.50*
Demolition waste from a plant (83% concrete, 13% masonry, 3% other)	*7.50*
Demolition waste from a plant (83% concrete, 13% masonry, 3% other)	*7.50*
Demolition waste from a plant (83% concrete, 13% masonry, 3% other)	*7.50*
Demolition waste from a plant (83% concrete, 13% masonry, 3% other)	*7.50*
Demolition waste from a plant (83% concrete, 13% masonry, 3% other)	*7.50*
Demolition waste from a plant (83% concrete, 13% masonry, 3% other)	*7.50*
Demolition waste from a plant (83% concrete, 13% masonry, 3% other)	*7.50*
Demolition waste from a plant (83% concrete, 13% masonry, 3% other)	*7.50*
Demolition waste from a plant (83% concrete, 13% masonry, 3% other)	*7.50*
Demolition waste from a plant (83% concrete, 13% masonry, 3% other)	*7.50*
n/a	*1.20*
n/a	*1.20*
n/a	*1.20*
n/a	*1.20*
n/a	*1.20*
n/a	*1.20*
Concrete waste (unknown origin)	*5.64*
Concrete waste (unknown origin)	*5.64*
Concrete waste (unknown origin)	*5.64*
Concrete waste (unknown origin)	*5.64*
Concrete waste (unknown origin)	*5.64*
Concrete waste (unknown origin)	*5.64*
Concrete waste (unknown origin)	*5.64*
Concrete waste (unknown origin)	*5.64*
Concrete waste (unknown origin)	*5.64*
Concrete waste (unknown origin)	*5.64*
Concrete waste (unknown origin)	*5.64*
Concrete waste (unknown origin)	*5.64*
Concrete waste (unknown origin)	*5.64*
Concrete waste (unknown origin)	*5.64*
Concrete waste (unknown origin)	*5.64*
Concrete waste (unknown origin)	*5.64*
n/a	*0.60*

n/a	*0.60*
n/a	*0.60*
No data	*4.80*
No data	*4.80*
No data	*4.80*
No data	*4.80*
No data	*4.80*
No data	*4.80*
No data	*4.80*
No data	*4.80*
No data	*4.80*
n/a	*1.10*
n/a	*1.10*
Laboratory recycling of cubes	*6.53*
Laboratory recycling of cubes	*6.53*
Laboratory recycling of cubes	*5.56*
Laboratory recycling of cubes	*5.56*
Laboratory recycling of cubes	*4.95*
Laboratory recycling of cubes	*4.95*
Laboratory recycling of cubes	*4.57*
Laboratory recycling of cubes	*4.57*
Laboratory recycling of cubes	*3.87*
Laboratory recycling of cubes	*3.87*
n/a	*1.30*
n/a	*1.30*
Rejected precast elements	*6.90*
Rejected precast elements	*6.90*
Rejected precast elements	*6.40*
Rejected precast elements	*6.40*
n/a	*1.00*
n/a	*1.00*
Rejected precast elements	*5.40*
Rejected precast elements	*5.40*
Rejected precast elements	*5.80*
Rejected precast elements	*5.80*
n/a	*1.30*
n/a	*1.30*
Rejected precast elements	*4.20*
Rejected precast elements	*4.20*
Rejected precast elements	*4.20*
Rejected precast elements	*4.20*
n/a	*1.00*
n/a	*1.00*
Rejected precast elements	*3.60*
Rejected precast elements	*3.60*
Rejected precast elements	*3.90*
Rejected precast elements	*3.90*
n/a	*0.70*
n/a	*0.70*
From a plant, 79% concrete, 13% masonry, 2% asphalt, 6% other	*6.40*
From a plant, 79% concrete, 13% masonry, 2% asphalt, 6% other	*6.40*
From a plant, 79% concrete, 13% masonry, 2% asphalt, 6% other	*6.40*
From a plant, 79% concrete, 13% masonry, 2% asphalt, 6% other	*6.40*
n/a	*1.51*
n/a	*1.51*

Precast concrete elements	*4.63*
Precast concrete elements	*4.63*
Precast concrete elements	*4.63*
Precast concrete elements	*4.63*
n/a	*1.60*
n/a	*1.60*
Columns and beams of old buildings	*1.93*
Columns and beams of old buildings	*1.93*
Columns and beams of old buildings	*6.24*
Columns and beams of old buildings	*6.24*

Cement Type [2]	Admixture/ Additive 1	Ad. 1 (% of cem)	Admixture/ Additive 2	Ad. 2 (% of cem)	w/c_{eff}	$f_{cm,exp}$ (MPa)
42.5N	superplasticizer	0.33	n/a	n/a	0.60	42.02
42.5N	superplasticizer	0.33	n/a	n/a	0.60	42.02
42.5N	superplasticizer	0.33	n/a	n/a	0.60	42.02
42.5N	superplasticizer	0.33	n/a	n/a	0.60	42.86
42.5N	superplasticizer	0.33	n/a	n/a	0.60	42.86
42.5N	superplasticizer	0.33	n/a	n/a	0.60	42.86
42.5N	superplasticizer	0.33	n/a	n/a	0.60	42.51
42.5N	superplasticizer	0.33	n/a	n/a	0.60	42.51
42.5N	superplasticizer	0.33	n/a	n/a	0.60	42.51
42.5N	superplasticizer	0.33	n/a	n/a	0.60	40.86
42.5N	superplasticizer	0.33	n/a	n/a	0.60	40.86
42.5N	superplasticizer	0.33	n/a	n/a	0.60	40.86
42.5N	superplasticizer	0.53	n/a	n/a	0.50	50.17
42.5N	superplasticizer	0.53	n/a	n/a	0.50	50.17
42.5N	superplasticizer	0.53	n/a	n/a	0.50	50.17
42.5N	superplasticizer	0.53	n/a	n/a	0.50	51.59
42.5N	superplasticizer	0.53	n/a	n/a	0.50	51.59
42.5N	superplasticizer	0.53	n/a	n/a	0.50	51.59
42.5N	superplasticizer	0.53	n/a	n/a	0.50	51.64
42.5N	superplasticizer	0.53	n/a	n/a	0.50	51.64
42.5N	superplasticizer	0.53	n/a	n/a	0.50	51.64
42.5N	superplasticizer	0.53	n/a	n/a	0.50	50.30
42.5N	superplasticizer	0.53	n/a	n/a	0.50	50.30
42.5N	superplasticizer	0.53	n/a	n/a	0.50	50.30
42.5N	superplasticizer	0.70	n/a	n/a	0.50	49.40
42.5N	superplasticizer	0.70	n/a	n/a	0.50	49.40
42.5N	superplasticizer	0.70	n/a	n/a	0.50	49.40
42.5N	superplasticizer	0.80	n/a	n/a	0.50	49.00
42.5N	superplasticizer	0.80	n/a	n/a	0.50	49.00
42.5N	superplasticizer	0.80	n/a	n/a	0.50	49.00
42.5N	superplasticizer	1.10	n/a	n/a	0.50	47.10
42.5N	superplasticizer	1.10	n/a	n/a	0.50	47.10
42.5N	superplasticizer	1.10	n/a	n/a	0.50	47.10
42.5N	superplasticizer	1.50	n/a	n/a	0.50	43.20
42.5N	superplasticizer	1.50	n/a	n/a	0.50	43.20
42.5N	superplasticizer	1.50	n/a	n/a	0.50	43.20
42.5N	superplasticizer	0.70	n/a	n/a	0.65	41.60
42.5N	superplasticizer	0.70	n/a	n/a	0.65	41.60
42.5N	superplasticizer	0.70	n/a	n/a	0.65	41.60
42.5N	superplasticizer	1.00	n/a	n/a	0.65	40.50
42.5N	superplasticizer	1.00	n/a	n/a	0.65	40.50
42.5N	superplasticizer	1.00	n/a	n/a	0.65	40.50
42.5N	superplasticizer	1.50	n/a	n/a	0.65	38.80
42.5N	superplasticizer	1.50	n/a	n/a	0.65	38.80
42.5N	superplasticizer	1.50	n/a	n/a	0.65	38.80
42.5N	superplasticizer	2.00	n/a	n/a	0.65	35.80
42.5N	superplasticizer	2.00	n/a	n/a	0.65	35.80
42.5N	superplasticizer	2.00	n/a	n/a	0.65	35.80
42.5R	n/a	n/a	n/a	n/a	0.43	51.00
42.5R	n/a	n/a	n/a	n/a	0.43	51.00
42.5R	n/a	n/a	n/a	n/a	0.43	51.00
42.5R	n/a	n/a	n/a	n/a	0.43	51.00

42.5R	n/a	n/a	n/a	n/a	0.43	48.80
42.5R	n/a	n/a	n/a	n/a	0.43	48.80
42.5R	n/a	n/a	n/a	n/a	0.43	48.80
42.5R	n/a	n/a	n/a	n/a	0.43	48.80
42.5R	n/a	n/a	n/a	n/a	0.43	51.30
42.5R	n/a	n/a	n/a	n/a	0.43	51.30
42.5R	n/a	n/a	n/a	n/a	0.43	51.30
42.5R	n/a	n/a	n/a	n/a	0.43	51.30
42.5R	n/a	n/a	n/a	n/a	0.43	51.20
42.5R	n/a	n/a	n/a	n/a	0.43	51.20
42.5R	n/a	n/a	n/a	n/a	0.43	51.20
42.5R	n/a	n/a	n/a	n/a	0.43	51.20
42.5R	superplasticizer	0.82	n/a	n/a	0.45	53.30
42.5R	superplasticizer	0.82	n/a	n/a	0.45	53.30
42.5R	superplasticizer	0.82	n/a	n/a	0.45	53.30
42.5R	superplasticizer	0.82	ge-reducing adı	2.74	0.45	47.30
42.5R	superplasticizer	0.82	ge-reducing adı	2.74	0.45	47.30
42.5R	superplasticizer	0.82	ge-reducing adı	2.74	0.45	47.30
42.5R	superplasticizer	0.82	n/a	n/a	0.45	51.10
42.5R	superplasticizer	0.82	n/a	n/a	0.45	51.10
42.5R	superplasticizer	0.82	n/a	n/a	0.45	51.10
42.5R	superplasticizer	0.82	ge-reducing adı	2.74	0.45	51.00
42.5R	superplasticizer	0.82	ge-reducing adı	2.74	0.45	51.00
42.5R	superplasticizer	0.82	ge-reducing adı	2.74	0.45	51.00
42.5R	superplasticizer	0.82	n/a	n/a	0.45	44.90
42.5R	superplasticizer	0.82	n/a	n/a	0.45	44.90
42.5R	superplasticizer	0.82	n/a	n/a	0.45	44.90
42.5R	superplasticizer	0.82	ge-reducing adı	2.74	0.45	51.10
42.5R	superplasticizer	0.82	ge-reducing adı	2.74	0.45	51.10
42.5R	superplasticizer	0.82	ge-reducing adı	2.74	0.45	51.10
4.25N	superplasticizer	0.70	n/a	n/a	0.50	45.25
4.25N	superplasticizer	0.70	n/a	n/a	0.50	45.25
4.25N	superplasticizer	0.70	n/a	n/a	0.50	45.25
4.25N	superplasticizer	0.70	n/a	n/a	0.50	45.25
4.25N	superplasticizer	0.70	n/a	n/a	0.50	45.25
4.25N	superplasticizer	0.70	n/a	n/a	0.50	45.25
4.25N	superplasticizer	0.70	n/a	n/a	0.50	47.40
4.25N	superplasticizer	0.70	n/a	n/a	0.50	47.40
4.25N	superplasticizer	0.70	n/a	n/a	0.50	47.40
4.25N	superplasticizer	0.70	n/a	n/a	0.50	47.40
4.25N	superplasticizer	0.70	n/a	n/a	0.50	47.40
4.25N	superplasticizer	0.70	n/a	n/a	0.50	47.40
4.25N	superplasticizer	0.70	n/a	n/a	0.50	47.30
4.25N	superplasticizer	0.70	n/a	n/a	0.50	47.30
4.25N	superplasticizer	0.70	n/a	n/a	0.50	47.30
4.25N	superplasticizer	0.70	n/a	n/a	0.50	47.30
4.25N	superplasticizer	0.70	n/a	n/a	0.50	47.30
4.25N	superplasticizer	0.70	n/a	n/a	0.50	47.30
4.25N	superplasticizer	1.40	n/a	n/a	0.50	54.80
4.25N	superplasticizer	1.40	n/a	n/a	0.50	54.80
4.25N	superplasticizer	1.40	n/a	n/a	0.50	54.80
4.25N	superplasticizer	1.40	n/a	n/a	0.50	54.80
4.25N	superplasticizer	1.40	n/a	n/a	0.50	54.80
4.25N	superplasticizer	1.40	n/a	n/a	0.50	54.80
42.5N	n/a	n/a	n/a	n/a	0.50	28.30

42.5N	n/a	n/a	n/a	n/a	0.50	28.30
42.5N	n/a	n/a	n/a	n/a	0.50	28.30
42.5N	n/a	n/a	n/a	n/a	0.50	32.30
42.5N	n/a	n/a	n/a	n/a	0.50	32.30
42.5N	n/a	n/a	n/a	n/a	0.50	32.30
42.5N	n/a	n/a	n/a	n/a	0.50	37.50
42.5N	n/a	n/a	n/a	n/a	0.50	37.50
42.5N	n/a	n/a	n/a	n/a	0.50	37.50
42.5N	n/a	n/a	n/a	n/a	0.50	30.90
42.5N	n/a	n/a	n/a	n/a	0.50	30.90
42.5N	n/a	n/a	n/a	n/a	0.50	30.90
42.5N	superplasticizer	?	n/a	n/a	0.50	45.00
42.5N	superplasticizer	?	n/a	n/a	0.50	45.00
42.5N	superplasticizer	?	n/a	n/a	0.50	35.00
42.5N	superplasticizer	?	n/a	n/a	0.50	35.00
42.5N	superplasticizer	?	n/a	n/a	0.50	40.00
42.5N	superplasticizer	?	n/a	n/a	0.50	40.00
42.5N	superplasticizer	?	n/a	n/a	0.50	42.00
42.5N	superplasticizer	?	n/a	n/a	0.50	42.00
42.5N	superplasticizer	?	n/a	n/a	0.50	45.00
42.5N	superplasticizer	?	n/a	n/a	0.50	45.00
42.5N	superplasticizer	?	n/a	n/a	0.50	45.00
42.5N	superplasticizer	?	n/a	n/a	0.50	45.00
42.5R	n/a	n/a	n/a	n/a	0.65	38.70
42.5R	n/a	n/a	n/a	n/a	0.65	38.70
42.5R	n/a	n/a	n/a	n/a	0.70	35.70
42.5R	n/a	n/a	n/a	n/a	0.70	35.70
42.5R	n/a	n/a	n/a	n/a	0.69	36.10
42.5R	n/a	n/a	n/a	n/a	0.69	36.10
42.5R	n/a	n/a	n/a	n/a	0.63	42.40
42.5R	n/a	n/a	n/a	n/a	0.63	42.40
42.5R	n/a	n/a	n/a	n/a	0.67	41.10
42.5R	n/a	n/a	n/a	n/a	0.67	41.10
42.5R	n/a	n/a	n/a	n/a	0.68	39.70
42.5R	n/a	n/a	n/a	n/a	0.68	39.70
42.5R	superplasticizer	1.00	n/a	n/a	0.41	71.10
42.5R	superplasticizer	1.00	n/a	n/a	0.41	71.10
42.5R	superplasticizer	1.00	n/a	n/a	0.46	66.80
42.5R	superplasticizer	1.00	n/a	n/a	0.46	66.80
42.5R	superplasticizer	1.00	n/a	n/a	0.45	68.50
42.5R	superplasticizer	1.00	n/a	n/a	0.45	68.50
42.5R	superplasticizer	1.00	n/a	n/a	0.40	72.30
42.5R	superplasticizer	1.00	n/a	n/a	0.40	72.30
42.5R	superplasticizer	1.00	n/a	n/a	0.43	70.20
42.5R	superplasticizer	1.00	n/a	n/a	0.43	70.20
42.5R	superplasticizer	1.00	n/a	n/a	0.45	66.50
42.5R	superplasticizer	1.00	n/a	n/a	0.45	66.50
42.5N	n/a	n/a	n/a	n/a	0.45	42.00
42.5N	n/a	n/a	n/a	n/a	0.45	42.00
42.5N	n/a	n/a	n/a	n/a	0.45	37.00
42.5N	n/a	n/a	n/a	n/a	0.45	37.00
42.5N	n/a	n/a	n/a	n/a	0.45	37.00
42.5N	n/a	n/a	n/a	n/a	0.45	37.00
42.5N	n/a	n/a	n/a	n/a	0.54	52.00
42.5N	n/a	n/a	n/a	n/a	0.54	52.00

42.5N	*n/a*	*n/a*	*n/a*	*n/a*	*0.54*	*50.00*
42.5N	*n/a*	*n/a*	*n/a*	*n/a*	*0.54*	*50.00*
42.5N	*n/a*	*n/a*	*n/a*	*n/a*	*0.54*	*48.00*
42.5N	*n/a*	*n/a*	*n/a*	*n/a*	*0.54*	*48.00*
42.5N	*superplasticizer*	*0.48*	*n/a*	*n/a*	*0.50*	*39.50*
42.5N	*superplasticizer*	*0.48*	*n/a*	*n/a*	*0.50*	*39.50*
42.5N	*superplasticizer*	*0.48*	*n/a*	*n/a*	*0.50*	*36.00*
42.5N	*superplasticizer*	*0.48*	*n/a*	*n/a*	*0.50*	*36.00*
42.5N	*superplasticizer*	*0.48*	*n/a*	*n/a*	*0.50*	*29.50*
42.5N	*superplasticizer*	*0.48*	*n/a*	*n/a*	*0.50*	*29.50*

Compressive strength specimen	f_{cm} (MPa)	f_{cm} RAC/NAC	$t–t_s$ (days)	t_s (days)	h_0 (mm)	RH (%)
cylinder Ø150/300 mm	42.02		28	1	50	50
cylinder Ø150/300 mm	42.02		90	1	50	50
cylinder Ø150/300 mm	42.02		180	1	50	50
cylinder Ø150/300 mm	42.86	1.02	28	1	50	50
cylinder Ø150/300 mm	42.86	1.02	90	1	50	50
cylinder Ø150/300 mm	42.86	1.02	180	1	50	50
cylinder Ø150/300 mm	42.51	1.01	28	1	50	50
cylinder Ø150/300 mm	42.51	1.01	90	1	50	50
cylinder Ø150/300 mm	42.51	1.01	180	1	50	50
cylinder Ø150/300 mm	40.86	0.97	28	1	50	50
cylinder Ø150/300 mm	40.86	0.97	90	1	50	50
cylinder Ø150/300 mm	40.86	0.97	180	1	50	50
cylinder Ø150/300 mm	50.17		28	1	50	50
cylinder Ø150/300 mm	50.17		90	1	50	50
cylinder Ø150/300 mm	50.17		180	1	50	50
cylinder Ø150/300 mm	51.59	1.03	28	1	50	50
cylinder Ø150/300 mm	51.59	1.03	90	1	50	50
cylinder Ø150/300 mm	51.59	1.03	180	1	50	50
cylinder Ø150/300 mm	51.64	1.03	28	1	50	50
cylinder Ø150/300 mm	51.64	1.03	90	1	50	50
cylinder Ø150/300 mm	51.64	1.03	180	1	50	50
cylinder Ø150/300 mm	50.30	1.00	28	1	50	50
cylinder Ø150/300 mm	50.30	1.00	90	1	50	50
cylinder Ø150/300 mm	50.30	1.00	180	1	50	50
cylinder Ø150/300 mm	49.40		28	28	50	50
cylinder Ø150/300 mm	49.40		56	28	50	50
cylinder Ø150/300 mm	49.40		100	28	50	50
cylinder Ø150/300 mm	49.00	0.99	28	28	50	50
cylinder Ø150/300 mm	49.00	0.99	56	28	50	50
cylinder Ø150/300 mm	49.00	0.99	100	28	50	50
cylinder Ø150/300 mm	47.10	0.95	28	28	50	50
cylinder Ø150/300 mm	47.10	0.95	56	28	50	50
cylinder Ø150/300 mm	47.10	0.95	100	28	50	50
cylinder Ø150/300 mm	43.20	0.87	28	28	50	50
cylinder Ø150/300 mm	43.20	0.87	56	28	50	50
cylinder Ø150/300 mm	43.20	0.87	100	28	50	50
cylinder Ø150/300 mm	41.60		35	28	50	50
cylinder Ø150/300 mm	41.60		63	28	50	50
cylinder Ø150/300 mm	41.60		100	28	50	50
cylinder Ø150/300 mm	40.50	0.97	35	28	50	50
cylinder Ø150/300 mm	40.50	0.97	63	28	50	50
cylinder Ø150/300 mm	40.50	0.97	100	28	50	50
cylinder Ø150/300 mm	38.80	0.93	35	28	50	50
cylinder Ø150/300 mm	38.80	0.93	63	28	50	50
cylinder Ø150/300 mm	38.80	0.93	100	28	50	50
cylinder Ø150/300 mm	35.80	0.86	35	28	50	50
cylinder Ø150/300 mm	35.80	0.86	63	28	50	50
cylinder Ø150/300 mm	35.80	0.86	100	28	50	50
cylinder Ø150/300 mm	51.00		7	1	75	60
cylinder Ø150/300 mm	51.00		28	1	75	60
cylinder Ø150/300 mm	51.00		56	1	75	60
cylinder Ø150/300 mm	51.00		90	1	75	60

cylinder Ø150/300 mm	*48.80*	*0.96*	*7*	*1*	*75*	*60*
cylinder Ø150/300 mm	*48.80*	*0.96*	*28*	*1*	*75*	*60*
cylinder Ø150/300 mm	*48.80*	*0.96*	*56*	*1*	*75*	*60*
cylinder Ø150/300 mm	*48.80*	*0.96*	*90*	*1*	*75*	*60*
cylinder Ø150/300 mm	*51.30*	*1.01*	*7*	*1*	*75*	*60*
cylinder Ø150/300 mm	*51.30*	*1.01*	*28*	*1*	*75*	*60*
cylinder Ø150/300 mm	*51.30*	*1.01*	*56*	*1*	*75*	*60*
cylinder Ø150/300 mm	*51.30*	*1.01*	*90*	*1*	*75*	*60*
cylinder Ø150/300 mm	*51.20*	*1.00*	*7*	*1*	*75*	*60*
cylinder Ø150/300 mm	*51.20*	*1.00*	*28*	*1*	*75*	*60*
cylinder Ø150/300 mm	*51.20*	*1.00*	*56*	*1*	*75*	*60*
cylinder Ø150/300 mm	*51.20*	*1.00*	*90*	*1*	*75*	*60*
cube 100/100/100 mm	*39.98*		*7*	*1*	*50*	*50*
cube 100/100/100 mm	*39.98*		*28*	*1*	*50*	*50*
cube 100/100/100 mm	*39.98*		*90*	*1*	*50*	*50*
cube 100/100/100 mm	*35.48*		*7*	*1*	*50*	*50*
cube 100/100/100 mm	*35.48*		*28*	*1*	*50*	*50*
cube 100/100/100 mm	*35.48*		*90*	*1*	*50*	*50*
cube 100/100/100 mm	*38.33*	*0.96*	*7*	*1*	*50*	*50*
cube 100/100/100 mm	*38.33*	*0.96*	*28*	*1*	*50*	*50*
cube 100/100/100 mm	*38.33*	*0.96*	*90*	*1*	*50*	*50*
cube 100/100/100 mm	*38.25*	*1.08*	*7*	*1*	*50*	*50*
cube 100/100/100 mm	*38.25*	*1.08*	*28*	*1*	*50*	*50*
cube 100/100/100 mm	*38.25*	*1.08*	*90*	*1*	*50*	*50*
cube 100/100/100 mm	*33.68*	*0.84*	*7*	*1*	*50*	*50*
cube 100/100/100 mm	*33.68*	*0.84*	*28*	*1*	*50*	*50*
cube 100/100/100 mm	*33.68*	*0.84*	*90*	*1*	*50*	*50*
cube 100/100/100 mm	*38.33*	*1.08*	*7*	*1*	*50*	*50*
cube 100/100/100 mm	*38.33*	*1.08*	*28*	*1*	*50*	*50*
cube 100/100/100 mm	*38.33*	*1.08*	*90*	*1*	*50*	*50*
cylinder Ø150/300 mm	*45.25*		*7*	*7*	*75*	*65*
cylinder Ø150/300 mm	*45.25*		*28*	*7*	*75*	*65*
cylinder Ø150/300 mm	*45.25*		*56*	*7*	*75*	*65*
cylinder Ø150/300 mm	*45.25*		*90*	*7*	*75*	*65*
cylinder Ø150/300 mm	*45.25*		*180*	*7*	*75*	*65*
cylinder Ø150/300 mm	*45.25*		*240*	*7*	*75*	*65*
cylinder Ø150/300 mm	*47.40*	*1.05*	*7*	*7*	*75*	*65*
cylinder Ø150/300 mm	*47.40*	*1.05*	*28*	*7*	*75*	*65*
cylinder Ø150/300 mm	*47.40*	*1.05*	*56*	*7*	*75*	*65*
cylinder Ø150/300 mm	*47.40*	*1.05*	*90*	*7*	*75*	*65*
cylinder Ø150/300 mm	*47.40*	*1.05*	*180*	*7*	*75*	*65*
cylinder Ø150/300 mm	*47.40*	*1.05*	*240*	*7*	*75*	*65*
cylinder Ø150/300 mm	*47.30*	*1.05*	*7*	*7*	*75*	*65*
cylinder Ø150/300 mm	*47.30*	*1.05*	*28*	*7*	*75*	*65*
cylinder Ø150/300 mm	*47.30*	*1.05*	*56*	*7*	*75*	*65*
cylinder Ø150/300 mm	*47.30*	*1.05*	*90*	*7*	*75*	*65*
cylinder Ø150/300 mm	*47.30*	*1.05*	*180*	*7*	*75*	*65*
cylinder Ø150/300 mm	*47.30*	*1.05*	*240*	*7*	*75*	*65*
cylinder Ø150/300 mm	*54.80*	*1.21*	*7*	*7*	*75*	*65*
cylinder Ø150/300 mm	*54.80*	*1.21*	*28*	*7*	*75*	*65*
cylinder Ø150/300 mm	*54.80*	*1.21*	*56*	*7*	*75*	*65*
cylinder Ø150/300 mm	*54.80*	*1.21*	*90*	*7*	*75*	*65*
cylinder Ø150/300 mm	*54.80*	*1.21*	*180*	*7*	*75*	*65*
cylinder Ø150/300 mm	*54.80*	*1.21*	*240*	*7*	*75*	*65*
cylinder Ø150/300 mm	*28.30*		*28*	*28*	*50*	*65*

cylinder Ø150/300 mm	28.30		90	28	50	65
cylinder Ø150/300 mm	28.30		200	28	50	65
cylinder Ø150/300 mm	32.30	1.14	28	28	50	65
cylinder Ø150/300 mm	32.30	1.14	90	28	50	65
cylinder Ø150/300 mm	32.30	1.14	200	28	50	65
cylinder Ø150/300 mm	37.50	1.33	28	28	50	65
cylinder Ø150/300 mm	37.50	1.33	90	28	50	65
cylinder Ø150/300 mm	37.50	1.33	200	28	50	65
cylinder Ø150/300 mm	30.90	1.09	28	28	50	65
cylinder Ø150/300 mm	30.90	1.09	90	28	50	65
cylinder Ø150/300 mm	30.90	1.09	200	28	50	65
cube 100/100/100 mm	33.75		28	3	35	50
cube 100/100/100 mm	33.75		112	3	35	50
cube 100/100/100 mm	26.25	0.78	28	3	35	50
cube 100/100/100 mm	26.25	0.78	112	3	35	50
cube 100/100/100 mm	30.00	0.89	28	3	35	50
cube 100/100/100 mm	30.00	0.89	112	3	35	50
cube 100/100/100 mm	31.50	0.93	28	3	35	50
cube 100/100/100 mm	31.50	0.93	112	3	35	50
cube 100/100/100 mm	33.75	1.00	28	3	35	50
cube 100/100/100 mm	33.75	1.00	112	3	35	50
cube 100/100/100 mm	33.75	1.00	28	3	35	50
cube 100/100/100 mm	33.75	1.00	112	3	35	50
cube 150/150/150 mm	30.57		28	?	75	60
cube 150/150/150 mm	30.57		90	?	75	60
cube 150/150/150 mm	28.20	0.92	28	?	75	60
cube 150/150/150 mm	28.20	0.92	90	?	75	60
cube 150/150/150 mm	28.52	0.93	28	?	75	60
cube 150/150/150 mm	28.52	0.93	90	?	75	60
cube 150/150/150 mm	33.50		28	?	75	60
cube 150/150/150 mm	33.50		90	?	75	60
cube 150/150/150 mm	32.47	0.97	28	?	75	60
cube 150/150/150 mm	32.47	0.97	90	?	75	60
cube 150/150/150 mm	31.36	0.94	28	?	75	60
cube 150/150/150 mm	31.36	0.94	90	?	75	60
cube 150/150/150 mm	56.17		28	?	75	60
cube 150/150/150 mm	56.17		90	?	75	60
cube 150/150/150 mm	52.77	0.94	28	?	75	60
cube 150/150/150 mm	52.77	0.94	90	?	75	60
cube 150/150/150 mm	54.12	0.96	28	?	75	60
cube 150/150/150 mm	54.12	0.96	90	?	75	60
cube 150/150/150 mm	57.12		28	?	75	60
cube 150/150/150 mm	57.12		90	?	75	60
cube 150/150/150 mm	55.46	0.97	28	?	75	60
cube 150/150/150 mm	55.46	0.97	90	?	75	60
cube 150/150/150 mm	52.54	0.92	28	?	75	60
cube 150/150/150 mm	52.54	0.92	90	?	75	60
cylinder Ø100/200 mm	40.95		28	7	37.5	55
cylinder Ø100/200 mm	40.95		90	7	37.5	55
cylinder Ø100/200 mm	36.08	0.88	28	7	37.5	55
cylinder Ø100/200 mm	36.08	0.88	90	7	37.5	55
cylinder Ø100/200 mm	36.08	0.88	28	7	37.5	55
cylinder Ø100/200 mm	36.08	0.88	90	7	37.5	55
cube 150/150/150 mm	41.08		28	1	50	50
cube 150/150/150 mm	41.08		90	1	50	50

cube 150/150/150 mm	*39.50*	*0.96*	*28*	*1*	*50*	*50*
cube 150/150/150 mm	*39.50*	*0.96*	*90*	*1*	*50*	*50*
cube 150/150/150 mm	*37.92*	*0.92*	*28*	*1*	*50*	*50*
cube 150/150/150 mm	*37.92*	*0.92*	*90*	*1*	*50*	*50*
cylinder Ø100/200 mm	*38.51*		*28*	*1*	*75*	*70*
cylinder Ø100/200 mm	*38.51*		*106*	*1*	*75*	*70*
cylinder Ø100/200 mm	*35.10*	*0.91*	*28*	*1*	*75*	*70*
cylinder Ø100/200 mm	*35.10*	*0.91*	*106*	*1*	*75*	*70*
cylinder Ø100/200 mm	*28.76*	*0.75*	*28*	*1*	*75*	*70*
cylinder Ø100/200 mm	*28.76*	*0.75*	*106*	*1*	*75*	*70*

ε_{cbs} (‰)	ε_{cds} (‰)	ε_{cs} (‰)	ε_{cs} RAC/NAC	Companion NAC Mix
n/a	n/a	0.200		n/a
n/a	n/a	0.305		n/a
n/a	n/a	0.332		n/a
n/a	n/a	0.231	1.16	C1-0
n/a	n/a	0.318	1.04	C1-0
n/a	n/a	0.345	1.04	C1-0
n/a	n/a	0.242	1.21	C1-0
n/a	n/a	0.368	1.21	C1-0
n/a	n/a	0.394	1.19	C1-0
n/a	n/a	0.242	1.21	C1-0
n/a	n/a	0.392	1.29	C1-0
n/a	n/a	0.414	1.25	C1-0
n/a	n/a	0.100		n/a
n/a	n/a	0.160		n/a
n/a	n/a	0.180		n/a
n/a	n/a	0.163	1.64	C2-0
n/a	n/a	0.196	1.22	C2-0
n/a	n/a	0.225	1.25	C2-0
n/a	n/a	0.163	1.64	C2-0
n/a	n/a	0.219	1.36	C2-0
n/a	n/a	0.241	1.34	C2-0
n/a	n/a	0.163	1.64	C2-0
n/a	n/a	0.308	1.92	C2-0
n/a	n/a	0.332	1.85	C2-0
n/a	n/a	0.210		n/a
n/a	n/a	0.284		n/a
n/a	n/a	0.345		n/a
n/a	n/a	0.252	1.20	NAC 0.5
n/a	n/a	0.331	1.17	NAC 0.5
n/a	n/a	0.402	1.17	NAC 0.5
n/a	n/a	0.294	1.40	NAC 0.5
n/a	n/a	0.393	1.38	NAC 0.5
n/a	n/a	0.470	1.36	NAC 0.5
n/a	n/a	0.343	1.63	NAC 0.5
n/a	n/a	0.487	1.71	NAC 0.5
n/a	n/a	0.574	1.66	NAC 0.5
n/a	n/a	0.242		n/a
n/a	n/a	0.295		n/a
n/a	n/a	0.338		n/a
n/a	n/a	0.230	0.95	NAC 0.65
n/a	n/a	0.309	1.05	NAC 0.65
n/a	n/a	0.338	1.00	NAC 0.65
n/a	n/a	0.264	1.09	NAC 0.65
n/a	n/a	0.336	1.14	NAC 0.65
n/a	n/a	0.370	1.09	NAC 0.65
n/a	n/a	0.338	1.39	NAC 0.65
n/a	n/a	0.414	1.40	NAC 0.65
n/a	n/a	0.477	1.41	NAC 0.65
n/a	n/a	0.072		n/a
n/a	n/a	0.166		n/a
n/a	n/a	0.206		n/a
n/a	n/a	0.235		n/a

n/a	*n/a*	*0.072*	*1.00*	*RC*
n/a	*n/a*	*0.185*	*1.11*	*RC*
n/a	*n/a*	*0.228*	*1.11*	*RC*
n/a	*n/a*	*0.261*	*1.11*	*RC*
n/a	*n/a*	*0.082*	*1.14*	*RC*
n/a	*n/a*	*0.205*	*1.23*	*RC*
n/a	*n/a*	*0.251*	*1.22*	*RC*
n/a	*n/a*	*0.286*	*1.22*	*RC*
n/a	*n/a*	*0.098*	*1.36*	*RC*
n/a	*n/a*	*0.243*	*1.46*	*RC*
n/a	*n/a*	*0.309*	*1.50*	*RC*
n/a	*n/a*	*0.360*	*1.53*	*RC*
n/a	*n/a*	*0.297*		*n/a*
n/a	*n/a*	*0.353*		*n/a*
n/a	*n/a*	*0.460*		*n/a*
n/a	*n/a*	*0.171*		*n/a*
n/a	*n/a*	*0.263*		*n/a*
n/a	*n/a*	*0.367*		*n/a*
n/a	*n/a*	*0.078*	*0.26*	*NAT+SP*
n/a	*n/a*	*0.180*	*0.51*	*NAT+SP*
n/a	*n/a*	*0.273*	*0.59*	*NAT+SP*
n/a	*n/a*	*0.128*	*0.75*	*NAT+SP+SRA*
n/a	*n/a*	*0.242*	*0.92*	*NAT+SP+SRA*
n/a	*n/a*	*0.348*	*0.95*	*NAT+SP+SRA*
n/a	*n/a*	*0.073*	*0.25*	*NAT+SP*
n/a	*n/a*	*0.195*	*0.55*	*NAT+SP*
n/a	*n/a*	*0.301*	*0.65*	*NAT+SP*
n/a	*n/a*	*0.055*	*0.32*	*NAT+SP+SRA*
n/a	*n/a*	*0.207*	*0.79*	*NAT+SP+SRA*
n/a	*n/a*	*0.324*	*0.88*	*NAT+SP+SRA*
n/a	*n/a*	*0.051*		*n/a*
n/a	*n/a*	*0.107*		*n/a*
n/a	*n/a*	*0.151*		*n/a*
n/a	*n/a*	*0.139*		*n/a*
n/a	*n/a*	*0.215*		*n/a*
n/a	*n/a*	*0.235*		*n/a*
n/a	*n/a*	*0.056*	*1.10*	*H40-A 0*
n/a	*n/a*	*0.111*	*1.04*	*H40-A 0*
n/a	*n/a*	*0.151*	*1.00*	*H40-A 0*
n/a	*n/a*	*0.144*	*1.03*	*H40-A 0*
n/a	*n/a*	*0.224*	*1.04*	*H40-A 0*
n/a	*n/a*	*0.248*	*1.05*	*H40-A 0*
n/a	*n/a*	*0.077*	*1.50*	*H40-A 0*
n/a	*n/a*	*0.127*	*1.19*	*H40-A 0*
n/a	*n/a*	*0.179*	*1.19*	*H40-A 0*
n/a	*n/a*	*0.169*	*1.22*	*H40-A 0*
n/a	*n/a*	*0.239*	*1.11*	*H40-A 0*
n/a	*n/a*	*0.262*	*1.11*	*H40-A 0*
n/a	*n/a*	*0.091*	*1.77*	*H40-A 0*
n/a	*n/a*	*0.172*	*1.61*	*H40-A 0*
n/a	*n/a*	*0.238*	*1.58*	*H40-A 0*
n/a	*n/a*	*0.218*	*1.56*	*H40-A 0*
n/a	*n/a*	*0.360*	*1.67*	*H40-A 0*
n/a	*n/a*	*0.399*	*1.70*	*H40-A 0*
n/a	*n/a*	*0.123*		*n/a*

n/a	*n/a*	*0.283*		*n/a*
n/a	*n/a*	*0.396*		*n/a*
n/a	*n/a*	*0.123*	*1.00*	*NAC*
n/a	*n/a*	*0.283*	*1.00*	*NAC*
n/a	*n/a*	*0.410*	*1.03*	*NAC*
n/a	*n/a*	*0.140*	*1.15*	*NAC*
n/a	*n/a*	*0.322*	*1.14*	*NAC*
n/a	*n/a*	*0.455*	*1.15*	*NAC*
n/a	*n/a*	*0.165*	*1.34*	*NAC*
n/a	*n/a*	*0.369*	*1.31*	*NAC*
n/a	*n/a*	*0.507*	*1.28*	*NAC*
n/a	*n/a*	*0.364*		*n/a*
n/a	*n/a*	*0.520*		*n/a*
n/a	*n/a*	*0.511*	*1.40*	*NA-I*
n/a	*n/a*	*0.700*	*1.35*	*NA-I*
n/a	*n/a*	*0.480*	*1.32*	*NA-I*
n/a	*n/a*	*0.655*	*1.26*	*NA-I*
n/a	*n/a*	*0.460*	*1.26*	*NA-I*
n/a	*n/a*	*0.638*	*1.23*	*NA-I*
n/a	*n/a*	*0.450*	*1.24*	*NA-I*
n/a	*n/a*	*0.615*	*1.18*	*NA-I*
n/a	*n/a*	*0.428*	*1.17*	*NA-I*
n/a	*n/a*	*0.596*	*1.15*	*NA-I*
n/a	*n/a*	*0.203*		*n/a*
n/a	*n/a*	*0.345*		*n/a*
n/a	*n/a*	*0.323*	*1.59*	*RC45PC*
n/a	*n/a*	*0.502*	*1.46*	*RC45PC*
n/a	*n/a*	*0.315*	*1.55*	*RC45PC*
n/a	*n/a*	*0.498*	*1.45*	*RC45PC*
n/a	*n/a*	*0.217*		*n/a*
n/a	*n/a*	*0.351*		*n/a*
n/a	*n/a*	*0.275*	*1.27*	*RC45PSC*
n/a	*n/a*	*0.463*	*1.32*	*RC45PSC*
n/a	*n/a*	*0.266*	*1.22*	*RC45PSC*
n/a	*n/a*	*0.469*	*1.34*	*RC45PSC*
n/a	*n/a*	*0.181*		*n/a*
n/a	*n/a*	*0.273*		*n/a*
n/a	*n/a*	*0.326*	*1.80*	*RC65PC*
n/a	*n/a*	*0.485*	*1.77*	*RC65PC*
n/a	*n/a*	*0.291*	*1.61*	*RC65PC*
n/a	*n/a*	*0.480*	*1.75*	*RC65PC*
n/a	*n/a*	*0.208*		*n/a*
n/a	*n/a*	*0.289*		*n/a*
n/a	*n/a*	*0.295*	*1.42*	*RC65PSC*
n/a	*n/a*	*0.465*	*1.61*	*RC65PSC*
n/a	*n/a*	*0.301*	*1.45*	*RC65PSC*
n/a	*n/a*	*0.500*	*1.73*	*RC65PSC*
n/a	*n/a*	*0.331*		*n/a*
n/a	*n/a*	*0.368*		*n/a*
n/a	*n/a*	*0.429*	*1.30*	*1*
n/a	*n/a*	*0.437*	*1.19*	*1*
n/a	*n/a*	*0.624*	*1.89*	*1*
n/a	*n/a*	*0.650*	*1.77*	*1*
n/a	*n/a*	*0.369*		*n/a*
n/a	*n/a*	*0.491*		*n/a*

n/a	*n/a*	*0.350*	*0.95*	*RC*
n/a	*n/a*	*0.500*	*1.02*	*RC*
n/a	*n/a*	*0.384*	*1.04*	*RC*
n/a	*n/a*	*0.572*	*1.16*	*RC*
n/a	*n/a*	*0.293*		*n/a*
n/a	*n/a*	*0.427*		*n/a*
n/a	*n/a*	*0.363*	*1.24*	*Control mix*
n/a	*n/a*	*0.513*	*1.20*	*Control mix*
n/a	*n/a*	*0.301*	*1.03*	*Control mix*
n/a	*n/a*	*0.563*	*1.32*	*Control mix*

References:

1. *Beltrán MG, Barbudo A, Agrela F, et al (2014) Effect of cement addition on the properties of re*
2. *Brand AS, Roesler JR, Salas A (2015) Initial moisture and mixing effects on higher quality rec*
3. *Castaño JO, Domingo A, Lazaro C (2009) A study on drying shrinkage and creep of recycled*
4. *Corinaldesi V (2010) Mechanical and elastic behaviour of concretes made of recycled-concret*
5. *Duan ZH, Poon CS (2014) Properties of recycled aggregate concrete made with recycled agg*
6. *Gómez-Soberón JM (2002) Shrinkage of concrete with replacement of aggregate with recycle*
7. *Ho NY, Lee YPK, Lim WF, et al (2013) Efficient utilization of recycled concrete aggregate in st*
8. *Sri Ravindrarajah R, Tam CT (1985) Properties of concrete made with crushed concrete as co*
9. *Tošić N (2018) Behaviour of reinforced concrete beams made with recycled and waste materi*
10. *Amorim P, De Brito J, Evangelista L (2012) Concrete made with coarse concrete aggregate: I*
11. *Corinaldesi V, Moriconi G (2010) Recycling of rubble from building demolition for low-shrinkag*
12. *Domingo A, Lázaro C, Gayarre FL, et al (2010) Long term deformations by creep and shrinkag*
13. *Fan Y, Xiao J, Tam VWY (2014) Effect of old attached mortar on the creep of recycled aggreg*
14. *Kou S, Poon C (2015) Effect of the quality of parent concrete on the properties of high perform*
15. *Pedro D, de Brito J, Evangelista L (2014) Performance of concrete made with aggregates rec*
16. *Shaikh FUA, Nguyen HL (2013) Properties of concrete containing recycled construction and d*
17. *Soares D, De Brito J, Ferreira J, Pacheco J (2014) Use of coarse recycled aggregates from p*
18. *Yang KH, Chung HS, Ashour AF (2008) Influence of type and replacement level of recycled ag*
19. *Seara-Paz S (2015) Efect of long-term deformations in structural flexural performance and bo*